

# PIP: Prototypes-Injected Prompt for Federated Class Incremental Learning

Muhammad Anwar Ma'sum\*  
University of South Australia  
Adelaide, Australia  
masmy039@mymail.unisa.edu.au

Mahardhika Pratama  
University of South Australia  
Adelaide, Australia  
dhika.pratama@unisa.edu.au

Savitha Ramasamy  
Institute of Infocomm Research  
Singapore, Singapore  
ramasamysa@i2r.a-star.edu.sg

Lin Liu  
University of South Australia  
Adelaide, Australia  
lin.liu@unisa.edu.au

Habibullah Habibullah  
University of South Australia  
Adelaide, Australia  
habibullah.habibullah@unisa.edu.au

Ryszard Kowalczyk  
University of South Australia  
Adelaide, Australia  
ryszard.kowalczyk@unisa.edu.au

## ABSTRACT

Federated Class Incremental Learning (FCIL) is a new direction in continual learning (CL) for addressing catastrophic forgetting and non-IID data distribution simultaneously. Existing FCIL methods call for high communication costs and exemplars from previous classes. We propose a novel rehearsal-free method for FCIL named prototypes-injected prompt (PIP) that involves 3 main ideas: a) prototype injection on prompt learning, b) prototype augmentation, and c) weighted Gaussian aggregation on the server side. Our experiment result shows that the proposed method outperforms the current state of the arts (SOTAs) with a significant improvement (up to 33%) in CIFAR100, MiniImageNet and TinyImageNet datasets. Our extensive analysis demonstrates the robustness of PIP in different task sizes, and the advantage of requiring smaller participating local clients, and smaller global rounds. For further study, source codes of PIP, baseline, and experimental logs are shared publicly in <https://github.com/anwarmaxsum/PIP>.

## KEYWORDS

prototypes injection, prompt, class incremental learning, federated

### ACM Reference Format:

Muhammad Anwar Ma'sum, Mahardhika Pratama, Savitha Ramasamy, Lin Liu, Habibullah Habibullah, and Ryszard Kowalczyk. 2018. PIP: Prototypes-Injected Prompt for Federated Class Incremental Learning. In *Proceedings of Make sure to enter the correct conference title from your rights confirmation emai (Conference acronym 'XX)*. ACM, New York, NY, USA, 20 pages. <https://doi.org/XXXXXXXX.XXXXXXX>

## 1 INTRODUCTION

Federated learning (FL) offers a collaborative approach for many clients to produce a shared global model while protecting their data privacy [26][17] [32]. FL has recently sparked a great deal of academic interest and achieved outstanding success in various

application areas, including medical diagnosis [15], autonomous vehicle [12], and wearable technology [4]. However, the majority of FL methods are designed for a static application scenario, assuming the target classes are fixed and known in advance. In real-world applications, the data are dynamic, allowing local clients to access unseen target classes online.

Existing studies have addressed dynamic data challenges in FL through Federated Class Incremental Learning (FCIL) where each local client gathers training data continually according to their continuous observation of the environment. In contrast, new clients with unforeseen classes are always welcome to join the FL training [8] [9] [41]. The clients have to cooperatively train a global model that continually learns new classes while maintaining its capability to recognize the previous classes. Despite its capability to learn new classes, the global model tends to lose its knowledge of previous classes known as catastrophic forgetting. Therefore, FCIL calls for answers on how to handle catastrophic forgetting in a dynamic collaborative continual learning, while preserving data privacy. In addition, the clients may carry non-independently and identically distributed (non-i.i.d.) data with imbalance classes.

The current FCIL state-of-the-art (SOTA) i.e. GLFC[9] and LGA[8] train and share whole backbone parameters resulting in a large number of parameters (11.3M) to train that requires a longer training time, and a high communication cost (61.7MB) as shown in Table 1. In addition, in the case of client-server limited communication costs e.g. due to limited bandwidth, this approach is forced to utilize a smaller (more shallow) model to reduce the shared parameter size. Second, in the current SOTAs, the clients privately share perturbed images with the central server for the aggregation process. Besides its inefficient size (16.5MB), sharing perturbed images may violate data privacy principles since perturbation doesn't guarantee information leakage. Furthermore, this mechanism can't answer the data openness problem, where the data is only open for a client at a specific moment. These intriguing gaps motivate us to develop a more efficient yet more effective approach to the FCIL problem, where a client trains and shares as small parameters as possible but produces a highly accurate global model without sharing any (perturbed) samples.

In this study, we propose a new approach named federated prompt for the FCIL problem that is implemented in our proposed baselines and our proposed method named prototype-injected prompt (PIP). In our proposed approach, a client trains and shares only a

Permission to make digital or hard copies of all or part of this work for personal or classroom use is granted without fee provided that copies are not made or distributed for profit or commercial advantage and that copies bear this notice and the full citation on the first page. Copyrights for components of this work owned by others than the author(s) must be honored. Abstracting with credit is permitted. To copy otherwise, or republish, to post on servers or to redistribute to lists, requires prior specific permission and/or a fee. Request permissions from [permissions@acm.org](mailto:permissions@acm.org).

Conference acronym 'XX, June 03–05, 2018, Woodstock, NY

© 2018 Copyright held by the owner/author(s). Publication rights licensed to ACM.

ACM ISBN 978-1-4503-XXXX-X/18/06

<https://doi.org/XXXXXXXX.XXXXXXX>

Method	B.Bone	Trainable Params		Prototype		Com. Cost(B)	
		Type	#N	Size(B)	Type		Size(B)
GLFC	ResNet18*	ResNet18*	11.3M	45.2 M	Perturbed Images*	16.5 M	61.7 M
LGA	ResNet18*	ResNet18*	11.3M	45.2 M	Perturbed Images*	16.5 M	61.7 M
Baseline (Ours)	ViT <sup>x</sup>	Prompt*	0.33M	1.32 M	-	-	1.32 M
PIP (Ours)	ViT <sup>x</sup>	Prompt*	0.33M	1.32 M	Deep Features*	0.03 M	1.35 M

**Table 1: The difference between our proposed approach and current SOTA in Federated Class Incremental Learning (FCIL), \* indicates sharable parameters, while <sup>x</sup> indicates unsharable parameters.**

small (0.33M) set of parameters called prompt, while the backbone model remains frozen and unsharable. In our approach, the bound for communication cost is only in the prompt size not in the backbone size. As an advantage, we could utilize any backbone with any complexity, number of parameters, and size. Our approach utilizes deep features as a shareable prototype to handle the non-i.i.d data between clients. As the second advantage, our approach offers far smaller prototypes (0.03MB) and guarantees data privacy as deep features represent a totally different structure and value compared to raw or perturbed samples. The key points difference between our approach and current SOTA is described in Table 1. **The contributions** of this paper are summarized as follows:

- We propose a new approach, prompt-based federated continual learning to solve the FCIL problem, where clients and central servers exchange prompts and head layer units instead of a whole model. This approach significantly reduces the size of the exchanged parameters between clients and the central server in each round.
- We propose a new baseline method for the FCIL problem named Federated DualPrompt (Fed-DualP) that already outperforms the current state-of-the-art (SOTA) methods in three benchmark datasets.
- We propose a novel method for the FCIL problem named Prototype-Injected Prompt (PIP) that consists of three main ideas i.e. a) prototype injection on prompt learning, b) prototype augmentation, and c) weighted Gaussian aggregation on the server side. The proposed method outperforms the baseline and current SOTAs with a significant gap.
- We provide a comprehensive analysis in three benchmark datasets as well as the robustness of the proposed method in different task sizes, smaller participating clients, and smaller rounds per task.
- The source codes of PIP are shared in <https://anonymous.4open.science/r/an122pouyyt789/> during the peer-review process and will be made public upon acceptance of our paper for further study and reproducibility.

## 2 RELATED WORKS

**a). Class Incremental Learning (CIL):** Prompt-based approach e.g. L2P [39], DualPrompt [38], CODA-Prompt [34] offers a breakthrough solution for CIL by training only small amounts of parameters called **prompt** for down-streaming tasks sequence, while the backbone model which contains the biggest parameter numbers stays frozen. This approach reduces the training time and offers utilization of a more complex backbone model e.g. ViT instead

of CNN. The rehearsal approach e.g. ICARL [30], EEIL, [7], GD [28], DER++ [6], trains exemplars (memory) from the previous task joined with current task samples to minimize model forgetting on previous tasks. This approach doesn't work well if the memory samples are not available. The bias correction approach e.g. BiC [40] and LUCIR [13] enhances the rehearsal approach by creating a task-wise bias layer to help the model achieve stability-plasticity balance in compensation to add extra parameters to be trained. The regularization approaches adaptively tune the base learner parameter to accommodate the previous task and current task e.g. EWC [18], MAS [2], LWF [23], DMC [44]. The regularization has the advantage that It works on memory-free CIL but on the contrary, it is outperformed by rehearsal and bias correction approaches if the memory is available. Prompt-based approach outperforms the other three approaches despite requiring no memory, but not yet been proven effective in a distributed (federated) setting.

**b). Federated Class Incremental Learning(FCIL):** The recent study on FCIL problem e.g. FedWeIT[41], GLFC [9], and LGA [8] strives to achieve an optimal global model by aggregating locally trained models sent by the clients. The current SOTAs are proven to be more effective than combining FedAvg [26] and class incremental learning approaches such as ICARL and BiC. However, as emphasized in Table 1, the current SOTAs train and share all backbone parameters, resulting in a less efficient training time and high communication costs. In Addition, the SOTAs assume that a client saves several exemplars as local memory and shares perturbed images with the server which is not always applicable in real applications. The other study i.e. TARGET [42] utilizes a synthetic dataset instead of saving exemplars from the previous tasks to train the whole backbone network. TARGET is proven to be more effective than Fed-LWF, Fed-EWC, and FedWeIT[41] but still outperformed by LGA and GLFC. Another approach i.e. FedCIL [29] uses a locally trained generative model i.e. ACGAN [27] to generate fake samples in the aggregation process. Despite its better performance than the combination of FedAvg or FedProx [20] with ACGAN, DGR[31] or LWF-2T [36] this method requires higher training time both in local and server-side and higher communication cost due to sending the generative model along with the backbone. To tackle the weaknesses above, our approach uses memory-free prompt learning for local training with the frozen backbone to achieve an efficient yet powerful local model, then aggregates the prompt and prototypes to obtain a generalized global model with low communication cost.

## 3 PRELIMINARIES

### 3.1 Problem Formulation

**Class incremental learning (CIL)** problem is defined as a learning problem of a sequence of fully supervised learning tasks  $\{\mathcal{T}^t\}_{t=1}^T$  where  $T$  represents the number of consecutive tasks, the value of  $T$  is unknown to the model before CIL process and can be infinite. Each task carries  $N_t$  pairs of training samples  $\mathcal{T}^t = \{x_i^t, y_i^t\}_{i=1}^{N_t}$  where  $x_i \in \mathcal{X}^t$  denotes input image and  $y_i \in \mathcal{Y}^t$  denotes its corresponding class label. Each task carries the same image size but possesses disjoint target classes to the other tasks. Suppose that

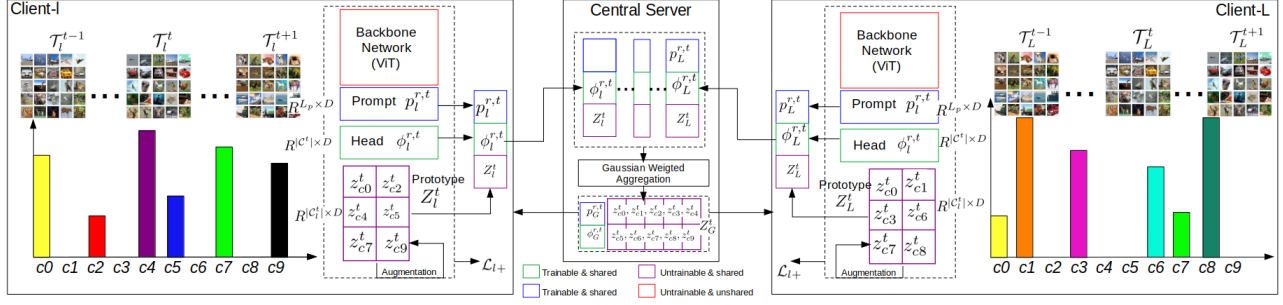


**Figure 1: Visualization of our proposed method (PIP) that includes prototypes-injected-prompt learning with  $\mathcal{L}_{l+}$  to handle local catastrophic forgetting, shared prototypes to handle non-i.i.d distributions between clients, prototypes augmentation to handle class-imbalance, and server Gaussian weighted aggregation to improve global model generalizations.**

$\mathcal{Y}^t$  is the labels set of task  $t$  and  $C^t$  denotes the unique class labels in  $\mathcal{Y}^t$ ,  $C^t = \{y_i^t, y_j^t \in \mathcal{Y}^t, i, j \in [1..N^t]\}_{\neq}$ , then we have  $\forall t, t' \in [1..T], t \neq t' \Rightarrow (\mathcal{Y}^t \cap \mathcal{Y}^{t'} = \emptyset) \wedge (C^t \cap C^{t'} = \emptyset)$ .

**Federated Class-Incremental Learning (FCIL)** is defined as: for  $r$ -th global round  $r \in [1..R]$ , a set of selected local clients  $\{S_l\}_{l=1}^L$  are conducting class incremental learning for the task  $t \in [1..T]$  with their local training set  $\{\mathcal{T}_l^t\}_{l=1}^L$  coordinated by a central server  $S_G$  in a federated manner, where  $R$  is the maximum global round. A client  $S_l$  may carry a unique set of a training set  $\mathcal{T}_l^t = \{x_{li}^t, y_{li}^t\}_{i=1}^{N_l^t}$ , which satisfies  $\forall l, l' \in [1..L], l \neq l' \Rightarrow (\mathcal{T}_l^t \neq \mathcal{T}_{l'}^t) \wedge (C_l^t \neq C_{l'}^t)$  where,  $N_l^t$  denotes number of training samples of client  $l$  for task  $t$ . FCIL satisfies  $\mathcal{T}^t = \cup_{l=1}^L \mathcal{T}_l^t$  and  $C^t = \cup_{l=1}^L C_l^t$ , therefore it satisfies  $C_l^t \subseteq C^t$  and  $|C_l^t| \leq |C^t|$ . Please note that  $\mathcal{T}_l^t$  is not shareable to another client  $S_{l'} (l \neq l')$  nor central server  $S_G$ . Clients may carry non-identically and distributed data (non-i.i.d), suppose that  $\mathcal{D}_l$  is the class distribution of  $l$ -th client, then it satisfies  $\forall l, l' \in [1..L], l \neq l' \Rightarrow (\mathcal{D}_l^t \neq \mathcal{D}_{l'}^t)$ . In each global round  $r$ -th for task  $t$ , each client  $S_l$  conducts local CIL training using its training samples  $\mathcal{T}_l^t$  optimizing its local model  $\Theta_l^{r,t}$ , then the clients send their local models to the central server  $S_G$ . The central server aggregates all participating local updated parameters  $\{\Theta_l^{r,t}\}_{l=1}^L$ , producing the latest global model parameter  $\Theta_G^{r,t}$ , then distributes it to all clients  $\{S_l\}_{l=1}^L$  for the next global round process.  $\Theta_l^{r,t}$  and  $\Theta_G^{r,t}$  denote the latest updated version of local parameter  $\Theta_l$  and global parameter  $\Theta_G$  respectively after  $r$ -th round of  $t$ -th task of FCIL training. Please note that a set of local clients  $\{S_l\}_{l=1}^L$  are randomly selected from all possibly participating clients simulating real-world conditions where only a small percentage of registered clients join in a round of federated learning.

### 3.2 Proposed Approach and Baselines: Federated Prompt-Based Continual Learning for FCIL

In prompt-based class incremental learning, a client uses a frozen backbone model e.g. Vision Transformer (ViT) as a feature extractor. The ViT embedding layer transforms an input image  $x \in R^{w \times h \times c}$ , where  $w, h, c$  are the image's width, height, and channel respectively, into sequence-like output feature  $h \in R^{L \times D}$ , where  $L$  is the

sequence length and  $D$  is the embedding dimension. A client only needs to update a small-sized trainable parameter called prompt  $p \in R^{L_p \times D}$  and its head layer parameter  $\phi$  to deal with the sequence of task  $\{\mathcal{T}_t\}_{t=1}^T$ ,  $L_p$  denotes the prompt length. Inspired by its effectiveness and efficiency in CIL problem, We proposed a federated prompt-based continual learning for the FCIL problem, where in a global round  $r$ -th for the  $t$ -th task a client  $S_l$  only updates its learnable parameters i.e. prompt  $p_l^{r,t} \in R^{L_p \times D}$ , and its classification (head) layer  $\phi_l^{r,t}$ , then send them to central server  $S_G$ . The central  $S_G$  aggregates accumulated parameters  $\{(p_l^{r,t}, \phi_l^{r,t})\}_{l=1}^L$  producing global model parameters  $(p_G^{r,t}, \phi_G^{r,t})$  and send it back to all clients. The size of  $(p_l^{r,t}, \phi_l^{r,t})$  is far smaller than the whole model  $\Theta_l = (\theta, \phi)$ . Therefore our proposed approach is more efficient both in terms of local training process and communication costs. The main distinction between our proposed approach and the existing state-of-the-art (SOTA) methods is that the SOTA methods train the whole model parameters  $\Theta = (\theta, \phi)$  where a model is defined as  $F_{\Theta}(x) = f_{\phi}(g_{\theta}(x))$ ,  $g_{\theta}(\cdot)$  is feature extractor and  $f_{\phi}(\cdot)$  is classifier, while our approach trains only small-sized parameters i.e. prompt  $p$  and head layer  $\phi$ , and freezes the backbone  $\theta$ .

In this study, we propose two baseline methods i.e. Federated Learning to Prompt (Fed-L2P), and Federated DualPrompt (Fed-DualP) by customizing L2P [39], and DualP [38], for federated class incremental learning problems. The main role of the baselines is to demonstrate that our new approach is more effective and efficient than current SOTAs for FCIL problem. Second, the baselines show that our approach applies to any prompt structure that is demonstrated by two different prompt structures i.e. L2P and DualP. In addition, we proposed those two methods as new baselines for further study on FCIL problem. Following L2P and DualP structure, in our baselines, the local client's prompt  $p_l$  represented as  $p_l = \{(e_l^t, k_l^t)\}_{t=1}^T$  in Fed-L2P  $p_l = (g_l, \{(e_l^t, k_l^t)\}_{t=1}^T)$  in Fed-DualP, where  $p_l^t \in R^{L_p \times D}$  and  $e_l^t \in R^{L_p \times D}$  represent a task-specific prompt,  $g_l \in R^{L_p \times D}$  represents global prompt,  $k_l^t$  is the key associated with a task-specific prompt  $p_l^t$  or  $e_l^t$ , and  $T$  denotes the number of tasks of client  $S_l$ . The central server aggregates participating clients' parameters by performing FedAvg [26].

## 4 PROPOSED METHOD: PROTOTYPE-INJECTED PROMPT (PIP)

Our proposed method, as visualized in Figure 1 performs prompt learning on each client to handle local catastrophic forgetting (section 4.1), handling non-i.i.d distribution by applying shared prototype injection(section 4.2), handling class-imbalance by performing prototypes augmentation (section 4.3), and finally improving global model generalization by using weighted aggregation (section 4.4).

**The uniqueness** of our method is that we utilize prompt and prototype as the shared knowledge between clients and the central server. Second, we propose a prototype injection mechanism in local training to improve local model generalization. Third, we propose a weighted aggregation on the server side. Our proposed method is distinct from prompt-based methods e.g. Fed-CPrompt[3] and FCILPT[24] that shared and trained prompts only. Our proposed method is also distinguished from prototype-based FL methods e.g. FedProto [35] and CCVR [25] shared only prototypes to refine the local model or use the prototype as classifiers. Besides, FedProto and CCVR are developed for federated learning only, meaning the methods didn't address the catastrophic forgetting issue.

### 4.1 Handling Local Catastrophic Forgetting via Prompt Learning

On a round  $r - th$  of  $t - th$  task, each client  $S_l$  optimizes its local prompt  $p_l$  and head layer parameter  $\phi_l$  using its available training samples  $\mathcal{T}_l^{r,t}$ . Please note that  $p_l$  can be any prompt structure as mentioned in our baselines e.g. in L2P, DualPrompt, or another prompt structure. Given a pre-trained ViT backbone  $f$  with  $M$  Multi head Self-Attention (MSA), where  $h^{(i)}$ ,  $i = 1, 2, \dots, M$  represents the input for  $i - th$  MSA layer, suppose that a local client wants to attach a latest updated prompt  $p_l^{r,t}$  into the  $i - th$  MSA layer, the prompt instance  $p_l^{r,t}$  transform feature  $h^{(i)}$  via prompt function as defined in equation 1.

$$h_{p_l^{r,t}}^{(i)} = f_{prompt}(p_l^{r,t}, h^{(i)}) \quad (1)$$

Note that  $h_i$  is the extension of  $h$ , a sequence-like parameter produced by the ViT embedding layer for the  $i - th$  MSA layer. Prompt function  $f_{prompt}$  can be implemented by using prompt tuning ( $f_{prompt}^{Pro-T}$ ) [19] or prefix ( $f_{prompt}^{Pre-T}$ ) tuning [22] approaches as defined in equation 2 and 3.

$$f_{prompt}^{Pro-T}(p_l^{r,t}, h^{(i)}) = MSA([p_l^{r,t} \oplus h_Q^{(i)}], [p_l^{r,t} \oplus h_K^{(i)}], [p_l^{r,t} \oplus h_V^{(i)}]) \quad (2)$$

$$f_{prompt}^{Pre-T}(p_l^{r,t}, h^{(i)}) = MSA(h_Q^{(i)}, [p_l^{r,t} \oplus h_K^{(i)}], [p_l^{r,t} \oplus h_V^{(i)}]) \quad (3)$$

$$MSA(h_Q^{(i)}, h_K^{(i)}, h_V^{(i)}) = (h_1^{(i)} \oplus h_2^{(i)} \oplus \dots \oplus h_{m-1}^{(i)} \oplus h_m^{(i)}) W^O \quad (4)$$

$$\text{where } h_j^{(i)} = \text{Attention}(h_Q^{(i)} W_j^Q, h_K^{(i)} W_j^K, h_V^{(i)} W_j^V)$$

MSA function is defined as in equation 4 following [37] where  $h_Q^{(i)}$ ,  $h_K^{(i)}$ , and  $h_V^{(i)}$  are input query, key, and value, for  $i - th$  MSA layer,  $p_{IK}^{r,t} \in R^{L_{p/2} \times D}$  and  $p_{IV}^{r,t} \in R^{L_{p/2} \times D}$  are splits of  $p_l^{r,t}$ ,  $W^O$ ,  $W_j^Q$ ,  $W_j^K$ , and  $W_j^V$  are the projection matrices, and  $m$  is number of head,  $\oplus$  represents concatenation function, and in ViT  $h_Q^{(i)} = h_K^{(i)} = h_V^{(i)} = h^{(i)} \in R^{L \times D}$ . Given a pair of samples  $(x_{li}^t, y_{li}^t) \in \mathcal{T}_l^t$ , each client  $S_l$  trains its latest updated parameters  $p_l^{r,t}$  and  $\phi_l^{r,t}$  using  $\mathcal{L}_l$

as defined in equation 5, where  $\mathcal{L}$  represents cross-entropy loss,  $\mathcal{L}_m$  represents matching loss between sample  $x_{li}^t$  and key  $x_{li}^t$ ,  $\lambda$  represents a constant factor,  $f_{p_l}$  represents prompt function, and  $f_{\phi_l}$  represents of  $l - th$  client.

$$\mathcal{L}_l = \mathcal{L}(f_{\phi_l^{r,t}}(f_{p_l^{r,t}}(x_{li}^t, y_{li}^t))) + \lambda \mathcal{L}_m(x_{li}^t, k_{li}^{r,t}), (x_{li}^t, y_{li}^t) \in \mathcal{T}_l^t \quad (5)$$

$$\begin{aligned} p_l^{r,t} &\leftarrow p_l^{r,t} - \alpha \nabla \mathcal{L}_l \\ \phi_l^{r,t} &\leftarrow \phi_l^{r,t} - \alpha \nabla \mathcal{L}_l \end{aligned} \quad (6)$$

The client's parameters are updated using equation 6 where  $\alpha$  represents learning rate and  $\nabla \mathcal{L}_l$  represents gradient with respect to  $\mathcal{L}_l$ .

### 4.2 Shared Prototype Injection: What, Why and How?

We define a prototype set on the  $t - th$  task of a client  $S_l$  as  $Z_l^t = \{z_{lc}^t\}$ ,  $z_{lc}^t \in R^{1 \times D}$  is the prototype for class  $c \in C_l^t$ ,  $C_l^t$  is the available classes in  $\mathcal{T}_l^t$ , and  $D$  is the embedding dimension. Assuming that the prototype follows a Gaussian distribution  $z_{lc}^t \sim \mathcal{N}(\mu_{lc}^t, \Sigma_{lc}^t)$  and the prototype is considered as  $D$  disjoint uni-variate distribution, then we have  $z_{lc}^t \sim \mathcal{N}(\mu_{lc}^t, \sigma_{lc}^t{}^2)$  where  $\sigma_{lc}^t{}^2 = I_D \cdot \sigma_{lc,i}^t{}^2$ ,  $i \in \{1, 2, \dots, D\}$ ,  $I_D$  is identity matrix. Suppose that  $\mathcal{T}_{lc}^t = \{(x_{li}^t, y_{li}^t) \in \mathcal{T}_l^t, y_{li}^t = c\}$  is the samples of class- $c$  in  $\mathcal{T}_l^t$  and  $|\mathcal{T}_{lc}^t|$  is the number of samples in  $\mathcal{T}_{lc}^t$ , we compute the prototype  $z_{lc}^t$  properties by Eq. 7 and 8.

$$\mu_{lc}^t = \frac{1}{|\mathcal{T}_{lc}^t|} \sum_{i=1}^{|\mathcal{T}_{lc}^t|} f_{p_l^{r,t}}(x_{li}^t), x_{li}^t \in \mathcal{T}_{lc}^t \quad (7)$$

$$\sigma_{lc}^t{}^2 = \frac{1}{|\mathcal{T}_{lc}^t|} \sum_{i=1}^{|\mathcal{T}_{lc}^t|} (\mu_{lc}^t - f_{p_l^{r,t}}(x_{li}^t))^2, x_{li}^t \in \mathcal{T}_{lc}^t \quad (8)$$

Due to non-i.i.d data between clients, FCIL satisfies  $\mathcal{T}_l^t \subseteq (\mathcal{T}^t = \cup_{l=1}^L \mathcal{T}_l^t)$  and  $\forall l, l' \in [1..L], l \neq l' \Rightarrow (\mathcal{T}_l^t \neq \mathcal{T}_{l'}^t) \wedge (C_l^t \neq C_{l'}^t)$ . It implies a client only optimize  $p_l$  and  $\phi_l$  with regard to  $\mathcal{T}_l^t$  but not yet to  $\mathcal{T}^t$ . The client  $S_l$  only learns  $C_l^t$  but not  $\overline{C_l^t} = C^t - C_l^t$ , classes that exist in  $\mathcal{T}^t$  but not in  $\mathcal{T}_l^t$ . Meanwhile, we can't afford to share any exemplar sample  $(x_{li}^t, y_{li}^t)$  due to data privacy. Aggregating the prompts and head doesn't guarantee optimal global model  $(p_G^{r,t}, \phi_G^{r,t})$  for  $\mathcal{T}^t$  since in the next round, the participating clients and their available data may be different from the current rounds'  $\forall r, r' \in [1..R], \forall l \in [1..L], r \neq r' \Rightarrow (S_l^{r,t} \neq S_l^{r',t}) \wedge (\mathcal{T}_l^{r,t} \neq \mathcal{T}_l^{r',t})$ . Furthermore, training in too many rounds leads to catastrophic forgetting.

To handle this challenge, we propose prototype sharing between clients and the central server, where the server collects all clients' prototype  $\{Z_l^t\}_{l=1}^L$  then distributes global prototype  $Z_G^t = Z^t = \cup_{l=1}^L Z_l^t$ . The shared prototype set  $Z_l^t$  ensures each client learns  $\overline{C_l^t}$  via  $\overline{Z_l^t} = Z^t - Z_l^t$ , therefore each client has chances to learn all classes  $C^t$  in  $\mathcal{T}^t$ . Besides, the prototype set  $Z^t$  has a small size in comparison to prompt  $p_l$  or head layer  $\phi_l$  where  $z_c^t \in Z^t$  has the size of  $1 \times D$ , where  $D$  is the embedding dimension, and It doesn't contain any raw information as contained in an exemplar sample.

Now each client can enhance its local training by **injecting** the shareable prototype set  $Z^t$  into its training process by considering

$\mathcal{T}_l^t \cup (Z^t, C^t) \approx \mathcal{T}^t$ , where  $Z^t$  is the prototype feature set, and  $C^t$  acts as the label for the prototypes of all classes  $c \in C^t$ . Therefore, the loss function and parameters update of each client can be defined as in Eq. 9 and 10. In case the prototype is not yet available e.g. first round ( $r = 1$ ), a local model is updated using Eq. 5 and 6.

$$\mathcal{L}_{l+} = \mathcal{L}(f_{\phi_l^{r,t}}(f_{p_l^{r,t}}(x_{li}^t) \cup Z^t), y_{li}^t \cup C^t) + \lambda \mathcal{L}_m(x_l^t, k_l^{r,t}), (x_{li}^t, y_{li}^t) \in \mathcal{T}_l^t \quad (9)$$

$$\begin{aligned} p_l^{r,t} &\leftarrow p_l^{r,t} - \alpha \nabla \mathcal{L}_{l+} \\ \phi_l^{r,t} &\leftarrow \phi_l^{r,t} - \alpha \nabla \mathcal{L}_{l+} \end{aligned} \quad (10)$$

### 4.3 Handling Class Imbalance via Prototype Augmentation

We can simply assign  $z_c^t \in Z^t$  by  $\mu_c^t$  to generate a single prototype for class- $c$ . However, to handle classes imbalance between locally available classes and unavailable classes that are represented by the shared prototypes. we enrich the prototypes by using an augmentation. Suppose that  $x_{c_1}$  is the sample for class  $c_1 \in C_l^t$ ,  $z_{c_2}^t \in Z^t$  is the prototype of class  $c_2 \in \overline{C_l^t} = C^t - C_l^t$ ,  $c_1$  is locally available class, and  $c_2$  is locally the unavailable class in client- $l$ , then we have  $|x_{c_1}| \gg 1$ , while  $|z_{c_2}^t| = 1$ . The prototype augmentations create artificial prototypes that satisfy  $|z_{c_2}^t| \approx |x_{c_1}|$  as defined in equation 11 to generate  $m$  augmented prototypes for class- $c$  based on Gaussian distribution  $z_c^t \sim \mathcal{N}(\mu_c^t, \sigma_c^{t2})$ , and  $\beta$  is a random value in  $(0, 1)$  range.

$$\begin{aligned} z_c^t &= \{\mu_c^t\} \cup \{u_{ci}^t\}_{i=1}^m, \text{ where} \\ u_{ci}^t &= \mu_c^t + \beta \sigma_c^t, m \geq 1 \end{aligned} \quad (11)$$

### 4.4 Server Weighted Aggregation

We proposed weighted Gaussian aggregation on the server side to improve global model generalization. The aggregation treats clients' contribution to global aggregation proportionally based on their participation and their training sample size following best practice where a model that learns more produces more convergent weight. We consider clients to learn their local data and then produce Gaussian distributed local parameters. We define  $\omega_l = \rho_l^t |\mathcal{T}_l^t|$  as the weight of a client- $l$  on the  $t$ -th task, where  $\rho_l^t$  is the total of client- $l$  participation until  $t$ -th task and  $|\mathcal{T}_l^t|$  is the number of samples in  $\mathcal{T}_l^t$ . Given  $\{(p_l^{r,t}, \phi_l^{r,t}, Z_l^t)\}_{l=1}^L$  is a set of locally optimized parameters by selected local clients  $\{S_l\}_{l=1}^L$  on the  $r$ -th of  $t$ -th task, then the global parameters  $(p_G^{r,t}, \phi_G^{r,t})$  and  $Z_G^t$  are computed by Gaussian-based weighted aggregation as We define in Eq. 12-15. Equation The derivation of the proposed weighted aggregation in presented in our supplemental document. The pseudo-code of PIP is presented in algorithm 1, while the pseudocode of our proposed baselines is presented in our supplemental document.

$$p_G^{r,t} = \frac{1}{\sum_{l=1}^L \omega_l} \sum_{l=1}^L (p_l^{r,t} \omega_l) \quad (12)$$

$$\phi_G^{r,t} = \frac{1}{\sum_{l=1}^L \omega_l} \sum_{l=1}^L (\phi_l^{r,t} \omega_l) \quad (13)$$

$$\begin{aligned} z_{Gc}^t &= \mathcal{N}(\mu_{Gc}^t, \sigma_{Gc}^{t2}), \text{ where} \\ \mu_{Gc}^t &= \frac{1}{\sum_{l=1}^L a_{lc}^t \omega_l} \sum_{l=1}^L a_{lc}^t \mu_{lc}^t \omega_l \end{aligned} \quad (14)$$

$$\begin{aligned} \sigma_{Gc}^{t2} &= \frac{1}{\sum_{l=1}^L a_{lc}^t \omega_l} \sum_{l=1}^L a_{lc}^t (\mu_{lc}^{t2} + \sigma_{lc}^{t2}) \omega_l - \mu_{Gc}^{t2} \\ \text{where } a_{lc}^t &= 1, \text{ if } (\mu_{lc}^t \text{ exists}) \text{ else } = 0 \end{aligned} \quad (15)$$

---

#### Algorithm 1 PIP

- 1: **Input:** Number of clients  $N$ , number of selected local clients  $L$ , total number of rounds  $R$ , number of task  $T$ , local epochs  $E$ , batch size  $B$ .
  - 2: Distribute frozen ViT backbone  $f$  to all clients  $\{S_l\}_{l=1}^N$  and central server  $S_G$
  - 3: Initiate prompt, key, and head layer for all clients and central server  $p_G = p_l, \phi_G = \phi_l, l \in \{1..N\}$
  - 4:  $R_T \leftarrow R/T$ ,  $R_T$  represents round per task
  - 5: **for**  $t = 1 : T$  **do**
  - 6:   Init global and local prototypes  $Z_G^t = Z_l^t, Z^t = \emptyset$
  - 7:   **for**  $r = 1 : R_T$  **do**
  - 8:      $S_l \leftarrow$  randomly select  $L$  local clients from  $N$  total clients
  - 9:     **Clients execute:**
  - 10:     Receive global parameters i.e  $(p_G, Z_G^t, \phi_G)$
  - 11:     Assign local parameters  $(p_l, \phi_l, Z_l^t) \leftarrow (p_G, \phi_G, Z_G^t)$
  - 12:      $\mathcal{B} \leftarrow$  Split  $\mathcal{T}_l^t$  into  $B$  sized batches
  - 13:     **for**  $e = 1 : E$  **do**
  - 14:       **for**  $b = 1 : \mathcal{B}$  **do**
  - 15:          Compute feature  $f_{p_l}(x)$  as in Eq. (1) to (4)
  - 16:          Compute logits with prototypes  $f_{\phi_l}(f_{p_l}(x) \cup Z^t)$
  - 17:          Compute loss  $\mathcal{L}_{t+}$  as in Eq. (9)
  - 18:          Update local parameters  $(p_l, \phi_l)$  w.r.t  $\mathcal{L}_{t+}$  as in Eq. (10)
  - 19:       **end for**
  - 20:       **if**  $Z_l^t = \emptyset$  **then**
  - 21:          Compute prototype  $z_{lc}^t \sim \mathcal{N}(\mu_{lc}^t, \sigma_{lc}^{t2})$  as in Eq. (7)-(8)
  - 22:       **end if**
  - 23:       Augment and unify the prototypes as in Eq. (11)
  - 24:     **end for**
  - 25:     Compute prototype  $z_{lc}^t \sim \mathcal{N}(\mu_{lc}^t, \sigma_{lc}^{t2})$  as in Eq. (7)-(8)
  - 26:     Set  $Z_l^t = \{z_{lc}^t\} = \{(\mu_{lc}^t, \sigma_{lc}^{t2})\}$ , for class- $c$  available in  $\mathcal{T}_l^t$
  - 27:     Store local parameters  $(p_l, \phi_l, Z_l^t)$
  - 28:     Compute clients' weight  $\omega_l^t$
  - 29:     Send local parameters  $(p_l, \phi_l, Z_l^t)$  and weight  $\omega_l^t$  to server
  - 30:     **Server executes:**
  - 31:     Receives selected local clients parameters  $\{(p_l, \phi_l, Z_l^t)\}_{l=1}^L$
  - 32:     Aggregates parameters  $(p_G, \phi_G) \leftarrow (p_l, \phi_l)$  as in Eq. (12)-(13)
  - 33:     Aggregates prototypes  $Z_G^t \leftarrow Z_l^t$  as in Eq. (14)-(15)
  - 34:     Send global parameters  $(p_G, \phi_G, Z_G^t)$  to all clients
  - 35:    **end for**
  - 36: **end for**
  - 37: **Output:** Optimal Global parameters  $(p_G, \phi_G)$  and local parameters  $(p_l, \phi_l), l \in 1..N$
- 

## 5 THEORETICAL ANALYSIS

Let  $\theta = (p, \phi)$  is the trainable parameters and  $F(\theta) = \mathbb{E}[\mathcal{L}_{l+}(\mathcal{T}; \theta)] = \mathbb{E}[\mathcal{L}_{l+}(\mathcal{T}; (p, \phi))]$  is the expected loss function,  $k, E, R$ , and  $L_S$  is local iteration, local epoch, global round, and number of selected local clients respectively. We follow  $L$ -smooth and  $\mu$ -strongly convex  $F$ , random uniformly distributed batches,  $G$ -bounded uniformly

gradient assumptions, and decreasing learning rate as in [21],[5] as detailed below:

**Assumption 1:**  $F_1, \dots, F_l, \dots, F_{L_S}$  are all  $L$ -smooth: for all  $\theta$  and  $\theta'$ ,  $F_l(\theta) \leq F_l(\theta') + (\theta - \theta')^T \nabla F_l(\theta) + \frac{L}{2} \|\theta - \theta'\|_2^2$ .

**Assumption 2:**  $F_1, \dots, F_l, \dots, F_{L_S}$  are all  $\mu$ -strongly convex: for all  $\theta$  and  $\theta'$ ,  $F_l(\theta) \leq F_l(\theta') + (\theta - \theta')^T \nabla F_l(\theta) + \frac{\mu}{2} \|\theta - \theta'\|_2^2$ .

**Assumption 3:** Let  $\xi_l^k$  be the random uniformly sampled from  $l$ -th local data at  $k$ -th iteration. The variance of stochastic gradients in each client is bounded by:  $\mathbb{E}[\|\nabla F_l(\theta_l^k, \xi_l^k) - \nabla F_l(\theta_l^k)\|] \leq \sigma_l^2$  for  $l = 1, 2, \dots, L_S$

**Assumption 4:** The expected squared norm of stochastic gradients in each client is bounded by:  $\mathbb{E}[\|\nabla F_l(\theta_l^k, \xi_l^k)\|] \leq G^2$  for all  $l = 1, 2, \dots, L_S$  and  $k = 1, 2, \dots, K$  where  $K \in \mathbb{N}$ .

**Assumption 5:**  $\sum_{k=1}^{\infty} \alpha_l^k = \infty$  and  $\sum_{k=1}^{\infty} \alpha_l^{k^2} < \infty$  where  $\alpha_l^k$  is the learning rate of  $l$ -th client in  $k$ -th step training.

**Assumption 6:** The objective function  $F_l$  and SG satisfy the following conditions.

(a). The sequence of  $\{\theta_l^k\}$  is contained in an open space where  $F_l$  is bounded below by a scalar  $F_{inf}$

(b) Exist scalars  $v_G \geq v > 0$  so that for all  $k \in \mathbb{N}$  satisfy:

$$\begin{aligned} \nabla F_l(\theta_l^k)^T \mathbb{E}_{\xi_l^k} [g(\theta_l^k, \xi_l^k)] &\geq v \|\nabla F_l(\theta_l^k)\|_2, \text{ and} \\ \|\mathbb{E}_{\xi_l^k} [g(\theta_l^k, \xi_l^k)]\|_2 &\leq v_G \|\nabla F_l(\theta_l^k)\|_2. \end{aligned} \quad (16)$$

We state the following theorems:

**Theorem 1:**  $\liminf_{k \rightarrow \infty} \mathbb{E}[\|\nabla F(\theta_k)\|_2^2] = 0$

**Theorem 2:** Let Chose  $\kappa = L/\mu$ ,  $\delta = \max(8\kappa, E)$ ,  $\alpha_r = 2/(\mu(\delta + r))$ ,  $C = 4/L_S E^2 G^2$ ,  $\theta^1, \theta^R, \theta^*$  is the initial, last updated ( $R$ -th), and optimum parameter respectively,  $F^*$  is minimum value of  $F$  then:  $\mathbb{E}[F(\theta^R)] - F^* \leq \frac{\kappa}{(\delta + R - 1)} \left( \frac{2(B+C)}{\mu} + \frac{\mu\delta}{2} \mathbb{E}[\|\theta^1 - \theta^*\|] \right)$ .

**Theorem 3:** Given  $\theta^*$  and  $\theta$  are optimal parameter in  $\mathcal{T}_l^t \cup \mathcal{Z}^t$  and  $\mathcal{T}_l^t$  respectively, where  $\mathcal{T}_l^t \subset \mathcal{T}^t$ , where  $|\mathcal{T}_l^t|/|\mathcal{T}^t| = \eta \in (0, 1)$ , then at least there's  $\epsilon > 0$  that satisfy  $F(\theta; \mathcal{T}^t) - F(\theta^*; \mathcal{T}^t) \geq \epsilon$ . Theorem 1 and 2 prove PIP local training and federated convergence respectively, while theorem 3 proves PIP generalization. The detailed theoretical analysis, and derivations are presented in supplemental document.

## 6 EXPERIMENT RESULTS AND ANALYSIS

### 6.1 Experimental Setting

**Datasets:** Our experiment is conducted using three main benchmarks in FCIL i.e. split CIFAR100, split MiniImageNet, and split TinyImageNet. The CIFAR100 and MiniImageNet datasets each contain 100 classes while TinyImageNet is a dataset with 200 classes. We follow settings from [9] and [8] where the dataset is split equally into all tasks. In our main numerical result, The dataset is split into 10 tasks i.e. 10 classes per task for CIFAR100 and MiniImageNet, and 20 classes per task for the TinyImageNet dataset. In our further analysis, we investigate the performance of the proposed methods in different task sizes e.g.  $T=5$  and  $T=20$ .

**Benchmark Algorithms:** PIP is implemented in two version algorithms i.e. PIP-L2P and PIP-DualP with L2P and DualP prompt structure respectively, PIP-L2P and PIP-DualP are compared with 10 state-of-the-art algorithms: LGA [8], TARGET [43], GLFC[9], AFC[16]+FL, DyTox[11]+FL, SS-IL[1]+FL, GeoDL[33]+iCaRL[30]+FL,

DDE[14]+iCaRL[30]+FL, PODNet[10]+FL, BiC[40]+FL, iCaRL[30]+FL, and the proposed baseline models (FedL2P and Fed-DualP). We compare with Fed-CPrompt[3] in the CIFAR100 dataset since it reported evaluation in the CIFAR100 dataset only. We didn't include a performance report from FCILPT[24] since they use memory in their experiment which is different from our setting. Please note that we can't find the complete and runnable released code from both Fed-CPrompt and FCILPT to produce the results in our simulation.

**Experimental Details:** Our numerical study is executed under a single NVIDIA A100 GPU with 40 GB memory across 3 runs with different random seeds {2021,2022,2023}. Fed-L2P, Fed-DualP, PIP-L2P, and PIP-DualP train  $T$  number of prompts  $p \in R^{5 \times 768}$  and  $\phi \in R^{|C \times 768|}$  head layer, while the competitors train whole CNN models following their original implementation. Following [8] and [9], each experiment is simulated by 30 total clients and 1 global server, where in each round, 10 (33.33%) local clients are selected randomly. Each client randomly receives 60% ( $\eta = 0.6$ ) class label space. The total global round is set to 100, the local clients' epoch is set to 2, and the learning rate is set by choosing the best value from {0.02,0.002}. On each task, we evaluate average accuracy and forgetting from all learned tasks.

	Accuracy in each task (T) on CIFAR100 (T=10, @10classes/task)												
Method	1	2	3	4	4	6	7	8	9	10	Avg	PD	Imp
iCaRL+FL	89.0	55.0	57.0	52.3	50.3	49.3	46.3	41.7	40.3	36.7	51.8	52.3	36.2
BiC+FL	88.7	63.3	61.3	56.7	53.0	51.7	48.0	44.0	42.7	40.7	55.0	48.0	33.0
PODNet+FL	89.0	71.3	69.0	63.3	59.0	55.3	50.7	48.7	45.3	45.0	59.7	44.0	28.3
DDE+iCaRL+FL	88.0	70.0	67.3	62.0	57.3	54.7	50.3	48.3	45.7	44.3	58.8	43.7	29.2
GeoDL+iCaRL+FL	87.0	76.0	70.3	64.3	60.7	57.3	54.7	50.3	48.3	46.3	61.5	40.7	26.5
SS-IL+FL	88.3	66.3	54.0	54.0	44.7	54.7	50.0	47.7	45.3	44.0	54.9	44.3	33.1
DyTox+FL	86.2	76.9	73.3	69.5	62.1	62.7	58.1	57.2	55.4	52.1	65.4	34.1	22.7
AFC+FL	85.6	73.0	65.1	62.4	54.0	53.1	51.9	47.0	46.1	43.6	58.2	42.0	29.8
GLFC	90.0	82.3	77.0	72.3	65.0	66.3	59.7	56.3	50.3	50.0	66.9	40.0	21.1
LGA	89.6	83.2	79.3	76.1	72.9	71.7	68.4	65.7	64.7	62.9	73.5	26.7	14.6
TARGET	70.6	39.0	27.5	21.6	18.8	16.4	14.2	12.2	10.7	9.1	24.0	61.4	64.0
Fed-CPrompt	97.3	90.5	86.7	83.4	83.3	82.2	81.6	79.7	79.0	79.4	84.3	17.9	3.7
Fed-L2P (BL)	94.4	73.9	68.6	67.5	64.7	64.8	66.6	66.6	66.2	65.9	69.9	28.6	18.1
Fed-DualP (BL)	96.8	81.6	75.7	72.6	69.5	67.3	69.9	69.2	69.9	69.7	74.2	27.1	13.8
<b>PIP-L2P (Ours)</b>	95.4	90.1	86.7	84.7	82.9	80.9	80.1	79.5	78.5	77.5	83.6	17.9	4.4
<b>PIP-DualP (Ours)</b>	<b>98.7</b>	<b>92.9</b>	<b>89.4</b>	<b>87.6</b>	<b>87.0</b>	<b>85.3</b>	<b>85.2</b>	<b>84.8</b>	<b>84.8</b>	<b>84.3</b>	<b>88.0</b>	<b>14.4</b>	-

**Table 2:** Numerical results on CIFAR100 (T=10), "BL" denotes our proposed baseline, "Avg" denotes the average accuracy of all tasks, denotes performance drop, and "Imp" denotes improvement/gap of PIP-DualP compared to the respective method

### 6.2 Numerical Results

The numerical result of the consolidated algorithms is shown in tables 2 and 3. Except to Fed-CPrompt, The baseline method (Fed-DualP) already achieves higher average accuracy (Avg) than the SOTA methods with 1 – 13% improvement in accuracy. Fed-DualP also experiences a lower performance drop (PD) (19 – 27%) compared to the SOTA methods ( $\geq 26\%$ ) except in the CIFAR100 dataset vs. LGA. Fed-L2P achieves higher performance than SOTAs in MiniImageNet and TinyImageNet datasets with  $\geq 11\%$  gap, but lower performance in the CIFAR100 dataset. The proposed method (PIP-DualP) achieves the highest accuracy with  $\geq 10\%$  gap compared to the baseline method, and  $\geq 14\%$  gap compared to the competitor methods (except Fed-CPrompt). The proposed method also achieves the lowest performance drop with (10 – 13%) gap compared to the

Method	Accuracy in each task (T) on MiniImageNet (T=10, @10classes/task)												Accuracy in each task (T) on TinyImageNet (T=10, @20classes/task)													
	1	2	3	4	5	6	7	8	9	10	Avg	PD	Imp	1	2	3	4	5	6	7	8	9	10	Avg	PD	Imp
iCaRL+FL	74.0	62.3	56.3	47.7	46.0	40.3	37.7	34.3	33.3	32.7	46.5	41.3	44.6	63.0	53.0	48.0	41.7	38.0	36.0	33.3	30.7	29.7	28.0	40.1	35.0	46.1
BiC+FL	74.3	63.0	57.7	51.3	48.3	46.0	42.7	37.7	35.3	34.0	49.0	40.3	42.0	65.3	52.7	49.3	46.0	40.3	38.3	35.7	33.0	31.7	29.0	42.1	36.3	44.1
PODNet+FL	74.3	64.0	59.0	56.7	52.7	50.3	47.0	43.3	40.0	38.3	52.6	36.0	38.5	66.7	53.3	50.0	47.3	43.7	42.7	40.0	37.3	33.7	31.3	44.6	35.4	41.7
DDE+iCaRL+FL	76.0	57.7	58.0	56.3	53.3	50.7	47.3	44.0	40.7	39.0	52.3	37.0	38.7	69.0	52.0	50.7	47.0	43.3	42.0	39.3	37.0	33.0	31.3	44.5	37.7	41.8
GeoDL+iCaRL+FL	74.0	63.3	54.7	53.3	50.7	46.7	41.3	39.7	38.3	37.0	49.9	37.0	41.1	66.3	54.3	52.0	48.7	45.0	42.0	39.3	36.0	32.7	30.0	44.6	36.3	41.6
SS-IL+FL	69.7	60.0	50.3	45.7	41.7	44.3	39.0	38.3	38.0	37.3	46.4	32.4	44.6	62.0	48.7	40.0	38.0	37.0	35.0	32.3	30.3	28.7	27.0	37.9	35.0	48.4
DyTox+FL	76.3	68.3	64.8	58.6	45.4	41.3	39.7	37.1	36.2	35.3	50.3	41.0	40.7	73.2	66.6	48.0	47.1	41.6	40.8	37.4	36.2	32.8	30.6	45.4	42.6	40.8
AFC+FL	82.5	74.1	66.8	60.0	48.0	44.3	42.5	40.9	39.0	36.1	53.4	46.4	37.6	73.7	59.1	50.8	43.1	37.0	35.2	32.6	32.0	28.9	27.1	42.0	46.6	44.3
GLFC	73.0	69.3	68.0	61.0	58.3	54.0	51.3	48.0	44.3	42.7	57.0	30.3	34.0	66.0	58.3	55.3	51.0	47.7	45.3	43.0	40.0	37.3	35.0	47.9	31.0	38.4
LGA	83.0	74.2	72.3	72.2	68.1	65.8	64.0	59.6	58.4	57.5	67.5	25.5	23.5	70.3	64.0	60.3	58.0	55.8	53.1	47.9	45.3	39.8	37.3	53.2	33.0	33.1
TARGET	56.1	27.5	20.0	15.9	11.9	8.8	6.9	5.0	2.7	2.3	15.7	53.8	75.3	57.1	32.7	20.9	14.7	11.6	8.3	7.1	5.2	3.8	3.0	16.4	54.1	69.8
Fed-L2P (BL)	95.2	80.9	79.1	77.7	76.3	75.7	76.0	75.8	74.1	76.7	78.7	18.6	12.3	80.6	71.5	70.6	67.5	65.2	66.7	66.2	65.9	64.2	64.3	68.3	16.3	18.0
Fed-DualP (BL)	97.6	83.6	82.5	79.2	76.6	76.2	75.8	75.8	75.6	78.5	80.1	19.1	10.9	86.3	74.6	71.2	65.9	63.3	62.0	61.3	59.9	58.2	61.3	66.4	25.0	19.9
PIP-L2P (Ours)	96.1	91.9	89.6	88.9	88.2	88.2	87.4	87.2	85.5	85.7	88.9	10.5	2.2	85.4	84.0	83.5	84.5	83.3	83.7	82.3	81.3	79.8	77.4	82.5	7.9	3.7
PIP-DualP (Ours)	98.4	90.9	90.4	90.7	90.2	90.7	90.3	90.4	88.9	89.2	91.0	9.2	-	92.8	86.4	86.6	87.5	86.7	87.0	85.3	84.9	83.9	81.4	86.3	11.4	-

**Table 3: Numerical results on MiniImageNet and TinyImageNet (T=10), "BL" denotes our proposed baseline, "Avg" denotes the average accuracy of all tasks, "PD" denotes performance drop, and "Imp" denotes improvement/gap of PIP-DualP compared to the respective method**

Method	Average Forgetting on each Task										AVG
	1	2	3	4	5	6	7	8	9	10	
LGA	-	4.0	4.4	8.9	13.7	12.6	13.9	14.7	15.7	16.8	11.6
TARGET	-	-0.6	0.4	1.7	1.7	2.0	2.5	3.8	4.7	4.7	2.3
Fed-CPrompt	-	3.8	5.0	5.3	5.2	5.2	5.1	5.4	5.3	4.8	5.0
Fed-L2P	-	0.9	1.9	0.3	-0.4	-3.4	-5.0	-4.0	-3.2	-4.0	-1.9
Fed-DualP	-	-0.4	2.7	2.3	2.4	2.8	-0.9	0.6	0.4	0.6	1.2
PIP-L2P	-	2.3	4.7	5.1	6.0	6.5	6.0	6.4	6.4	8.4	5.8
PIP-DualP	-	1.3	1.5	1.9	2.3	3.1	2.9	2.4	2.5	2.8	2.3

**Table 4: Detailed average forgetting of the consolidated methods in CIFAR100 (T=10)**

Conf.	Prompt	Proto +Aug	W.Agg	Head	T1 (C=10)	T10 (C=100)	Avg	PD	Imp
A	✓				82.15	60.66	65.69	21.49	22.59
B	✓	✓			90.99	77.56	81.59	13.43	6.69
C	✓		✓		82.13	61.35	66.10	20.78	22.18
D	✓	✓	✓		91.37	78.47	82.41	12.90	5.87
E	✓			✓	96.60	70.68	75.38	25.92	12.90
F	✓	✓		✓	98.90	84.17	87.82	14.73	0.46
G	✓		✓	✓	98.60	69.94	72.57	28.66	15.71
PIP	✓	✓	✓	✓	98.60	84.60	88.28	14.00	-

**Table 5: Ablation study on CIFAR100 dataset in one-seeded run i.e. 2021 using DualP prompt structure. "Avg" denotes the average accuracy of all tasks, "PD" denotes performance drop, and "Imp" denotes improvement/gap of PIP compared to the respective configuration**

baseline and  $\geq 12\%$  gap compared to the competitor methods. The table shows that PIP achieves a higher gap in TinyImageNet which is a relatively more complex problem than in MiniImageNet and CIFAR100. Compared to Fed-CPrompt, our proposed method achieve a higher accuracy and lower performance drop with a significant margin i.e.  $\geq 3\%$

Looking at performance on each task, tables 2, and 3 show that PIP-DualP achieves the highest accuracy in all tasks in those three datasets. In the first task, the proposed method achieves higher

performance with a small gap 1 – 4% gap compared to the baseline method. However, with the increasing number of tasks, the gap gets higher e.g. 5 – 12% in task-2, 5 – 20% in task-3, and 6 – 20% in task-10 (last task). It shows that the proposed method handles catastrophic forgetting better than the baseline method. PIP-L2P achieves second-best performance in all tasks except in the first task of the CIFAR100 dataset.

### 6.3 Forgetting Analysis

Table 4 shows the average forgetting of the consolidated methods in each task T. The table shows that our proposed method (PIP-DualP) achieves smaller average forgetting than existing SOTAs i.e. LGA and Fed-CPrompt with a significant gap i.e. 2.7% and 9.3% margin respectively. Fed-DualP achieves a comparable average forgetting with TARGET, but looking at the trend, TARGET forgetting is increasing along with the number of tasks, while PIP-DualP forgetting is relatively stable. Please note that TARGET achieves lower average accuracy than PIP-DualP with a 64% gap. Our baselines i.e. Fed-DualP and Fed-L2P archives have lower average forgetting than PIP-DualP despite achieving lower accuracy than PIP-DualP with a huge gap i.e. ( $> 13\%$ ). This shows that the baselines achieve better stability (old task accuracy) but in exchange struggle to achieve plasticity (new task accuracy).

### 6.4 Ablation Study

We conducted an ablation study to investigate the contribution of each component of the proposed method. The result is summarized in Table 5, while the detailed result is presented in our supplemental document. The result shows that the prototype and augmentation contribute the most to the improvement of the performance as shown by the performance difference of configurations E vs. F (12%), and G vs. H (16%). The weighted aggregation improves performance up to 1% as shown by the performance difference of PIP and configuration F. The head layer aggregation also plays an important role in the proposed method as shown that the absence of this component decreases performance with  $\geq 6\%$  margin. The absence of two components e.g. prototype and head aggregation

(configuration C) or prototype and weighted aggregation (configuration E) impact significantly the performance with 22% and 13% accuracy drop respectively. The absence of three components i.e. prototype, weighted aggregation, and head aggregation (configuration A) cost a 23% performance drop in the method.

## 6.5 Further Analysis

**a) Different task size:** We evaluate the performance of the proposed method compared to the competitor methods in different task sizes i.e.  $T=5$  and  $T=20$  to further investigate the robustness of the proposed method. Figure 2 summarizes the performance of the consolidated methods in CIFAR100, MiniImageNet, and TinyImageNet with  $T=5$  (upper figures) and  $T=20$  (bottom figures). The detailed numerical result is presented in our supplemental document.. Both in  $T=5$  and  $T=20$  settings, PIP-DualP achieves the highest performance almost in every task in all configurations. It achieves a slightly lower performance than PiP-L2P in the last 3 tasks of CIFAR100 with  $T=5$ . Besides, all figures show that the proposed method has gentle slopes compared to the baseline and competitor methods. It shows that the proposed method experiences the lowest performance drop from  $t_{th}$  to  $t + 1_{th}$  task. It confirmed the robustness of the proposed method in different task-size settings. The baseline (Fed-DualP) method achieves better accuracy than the competitor methods in all 6 settings, except in CIFAR100 with the  $T=5$  setting. In CIFAR100 with the  $T=5$  setting, the baseline method achieves higher performance in task-1 and task-5, but lower performance in task-3, and comparable performance in task-2 and task-4. It shows the promising idea of the federated prompt-based approach for the FCIL problem.

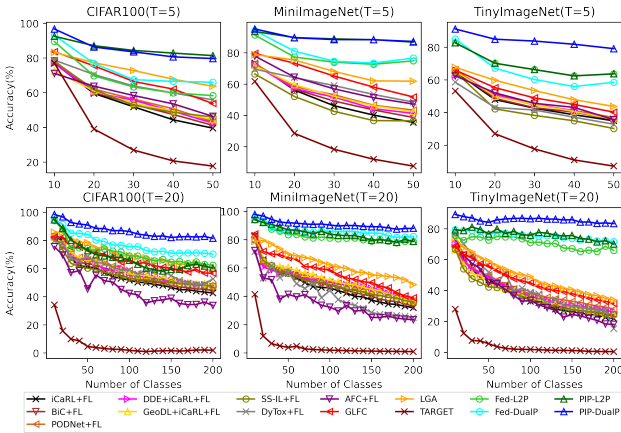


**Figure 2: Performance of the consolidated methods in CIFAR100, MiniImageNet and TinyImageNet with  $T=5$  and  $T=20$ .**

**b) Small local clients:** We evaluate the performance of the proposed method in smaller selected local clients to advance our investigation of the robustness of the proposed method on smaller selected local clients. This simulates cross-device federated learning where in a round only a small portion of registered clients participate in the federated learning process. In our experiment with 30

Method	CIFAR100 (T=10)			TinyImageNet (T=10)		
	L=10 (33.3%)	L=3 (10%)	L=2 (6.67%)	L=10 (33.3%)	L=3 (10%)	L=2 (6.67%)
GLFC	66.92	62.42	57.39	47.89	34.89 <sup>o</sup>	32.77 <sup>o</sup>
LGA	73.45	68.87	66.68	53.18	60.61*	58.54*
TARGET	24.00	14.19	14.18	16.43	9.34	7.56
Fed-L2P	70.86	71.94	71.09	70.02	69.16	65.25
Fed-DualP	83.10	75.08	64.68	67.31	66.11	67.03
PIP-L2P	75.38	76.96	72.17	82.85	79.23	76.17
PIP-DualP	88.28	87.06	83.78	86.79	85	82.13

**Table 6: Performance of the consolidated methods in CIFAR100 and TinyImageNet with smaller selected local clients (L), <sup>o</sup> and \* denote the results obtained from the first 4 and 5 tasks due to crash.**

total clients, we investigate the performance of the consolidated methods with 3 (10%) and 2 (6.67%) selected clients compared with the default setting with 10 clients (33.33%). Table 6 shows the performance of the consolidated methods in smaller local clients scenarios, while the complete result is presented in our supplemental document. The figure shows that the proposed methods experience the lowest performance degradation in fewer local clients. The figures show that both in CIFAR100 and TinyImageNet datasets, the proposed method still achieves higher accuracy than the baseline and the competitor methods with 10 participating local clients.

**c) Small global rounds:** We continue the previous experiment in smaller selected local clients into smaller local clients with smaller global rounds to study the robustness of the proposed method on a more extreme condition. This scenario simulates a condition where the model is urgently needed by the clients. In our experiment, we use 30 total clients and 3 (10%) local clients. Figure 3 summarizes our investigation on the performance of the proposed methods with 20 to 100 (default) global rounds in CIFAR100 and TinyImageNet datasets, while the complete result is presented in our supplemental document. The figure shows a common trend that the performance of the method is decreasing with the decreasing of global rounds. However, our proposed methods (PIP-DualP and PIP-L2P) experience a relatively small amount of performance drop with the decreasing global rounds. Meanwhile, the baseline method experiences a significant drop in the CIFAR100 dataset when the number of global rounds is reduced to 20. Besides, It may experience over-fitting when the number of global rounds is too high as shown by the result on the TinyImageNet dataset. Compared to the current SOTA (GLFC and LGA) methods with the default number of global rounds (100), PIP-DualP still achieves higher performance, even though the number of global rounds is reduced to 20 (20% default setting).

## 6.6 Complexity and Running Time Analysis

Following the pseudo-code in Algorithm 1, PIP generates prototypes when its prototype set is empty after a local epoch of a round- $r$  (line 21), augment the prototypes in each local epoch (23), and updates the prototypes after local epochs (line 26-27). Knowing that generating prototypes from  $\mathcal{T}_l^{r,t}$  costs  $O(N_l^t)$ , augmenting the

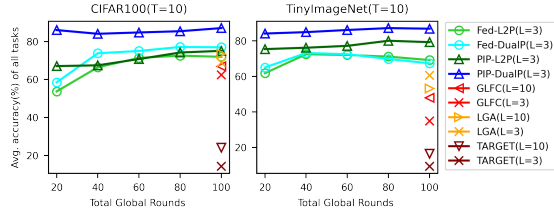


**Figure 3: Performance of the consolidated methods in CIFAR100 and TinyImageNet with smaller local clients (L) and smaller rounds.**

prototypes costs  $O(1)$  since it runs  $m \in \{1..5\}$  times, then the PIP complexity will be:

$$O(PIP) = O(1) + T.R_T.(O(\text{clients}) + O(\text{server})) \quad (17)$$

$$O(PIP) = O(1) + T.R_T.(L.O(1\text{-client}) + O(\text{server})) \quad (18)$$

$$O(PIP) = O(1) + T.R_T.(L.O(1\text{-client}) + O(1)) \quad (19)$$

$$O(PIP) = O(1) + T.R_T.L.O(E.(\sum_{b=1}^{\beta} N_{bl}^t + N_l^t) + O(N_l^t) + O(1)) + O(T.R_T) \quad (20)$$

Since we have  $\sum_{b=1}^{\beta} N_{bl}^t = N_l^t$ , then we have

$$O(PIP) = O(1) + T.R_T.L.O(E.(N_l^t + N_l^t) + O(N_l^t) + O(1)) + O(T.R_T) \quad (21)$$

$$O(PIP) = O(1) + T.R_T.L.O(E.N_l^t) + O(N_l^t) + O(1) + O(T.R_T) \quad (22)$$

$$O(PIP) = O(1) + O(T.R_T.L.E.N_l^t) + O(T.R_T.L.N_l^t) + O(T.R_T.L) + O(T.R_T) \quad (23)$$

$$O(PIP) = O(T.R_T.L.E.N_l^t) + O(T.R_T.L.N_l^t) + O(T.R_T.L) + O(T.R_T) \quad (24)$$

Substituting the equalities in the previous definition that  $R_T = R/T$  and  $N_l = T.N_l^t = T$  the complexity of PIP will be

$$O(PIP) = O(T.R/T.L.E.N_l^t) + O(T.R/T.L.N_l^t) + O(T.R/T.L) + O(T.R/T) \quad (25)$$

$$O(PIP) = O(R.L.E.N_l^t) + O(R.L.N_l^t) + O(R.L) + O(R) \quad (26)$$

$$O(PIP) = O(R.L.E.N_l^t) \quad (27)$$

Since  $N_l^t < N_l$  and E is set as a small constant in our method i.e. 2, then the PIP complexity will be:

$$O(PIP) = O(R.L.N_l) \quad (28)$$

The baseline's complexity is presented in the supplemental document. Our complexity analysis shows that both the baseline method and our proposed method have the same complexity i.e.  $O(R.L.N_l)$  where  $R$  is the number of global rounds,  $L$  is the number of participating local clients in each round, and  $N_l$  is the size of the training data in each client. Table 7 summarizes the training time of the consolidated method in three datasets with  $T=10$ . The table shows that the proposed method requires lower training time and far lower communication cost than the current competing SOTAs i.e. LGA and GLFC in all datasets. The training time is higher than the baseline training time because in our proposed method there are

additional processes that do not exist in the baseline i.e. prototype generation, augmentation, injection (concatenation with prompt features), aggregation, and feedback. TARGET may achieve the smallest running time, but It has poor performance with more than 60% margin compared to our proposed method in all datasets.

Method	Com.Cost	CIFAR100	MiniImageNet	TinyImagenet
GLFC	61.7 MB	24.3h	36.6h	46.4h
LGA	61.7 MB	23.2h	35.7h	45.9h
TARGET	69.8 MB	2.4h	2.3h	3.4h
Fed-L2P	0.49 MB	5.1h	6.6h	15.3h
Fed-DualP	1.32 MB	11.3h	11.1h	19.5h
PIP-L2P	0.52 MB	7.5h	8.0h	17.8h
PIP-DualP	1.35 MB	13.0h	14.5h	25.5h

**Table 7: Training time of the consolidated algorithm in CIFAR100, MiniImageNet and TinyImageNet.**

## 7 CONCLUDING REMARKS

In this paper, we propose a new approach named prompt-based federated learning, new baselines named Fed-L2P and Fed-DualP, and a novel method named prototype-injected prompt (PIP) for the FCIL problem. PIP consists of three main ideas: a) prototype injection on prompt, b) prototype augmentation, and c) weighted Gaussian aggregation on the server side. Our experimental result shows that the proposed method outperforms the current SOTAs with a significant gap (up to 33%) in CIFAR100, MiniImageNet, and TinyImageNet datasets. Our extensive analysis demonstrates the robustness of our proposed method in different task sizes, smaller participating local clients, and smaller global rounds. Our proposed method has the same complexity as the baseline method and experimentally requires shorter training time than the current SOTAs. In practice, our proposed method can be applied in both cross-silo and cross-domain federated class incremental learning. Our future work is directed to federated few-shot class incremental learning where each client only holds a few samples for each task.

## 8 ACKNOWLEDGEMENT

Muhammad Anwar Ma'sum acknowledges the support of Tokopedia-UI Centre of Excellence for GPU access to run the experiments. Savitha Ramasamy acknowledges the support of the National Research Foundation, Singapore under its AI Singapore Programme (AISG Award No: AISG2-RP-2021-027)

## REFERENCES

- [1] Hongjoon Ahn, Jihwan Kwak, Subin Lim, Hyeonsu Bang, Hyojun Kim, and Taesup Moon. 2021. Ss-il: Separated softmax for incremental learning. In *Proceedings of the IEEE/CVF International conference on computer vision*. 844–853.
- [2] Rahaf Aljundi, Francesca Babiloni, Mohamed Elhoseiny, Marcus Rohrbach, and Tinne Tuytelaars. 2018. Memory aware synapses: Learning what (not) to forget. In *Proceedings of the European conference on computer vision (ECCV)*. 139–154.
- [3] Gaurav Bagwe, Xiaoyong Yuan, Miao Pan, and Lan Zhang. 2023. Fed-cprompt: Contrastive prompt for rehearsal-free federated continual learning. *arXiv preprint arXiv:2307.04869* (2023).
- [4] Marc Jayson Baucas, Petros Spachos, and Konstantinos N Plataniotis. 2023. Federated learning and blockchain-enabled fog-IoT platform for wearables in predictive healthcare. *IEEE Transactions on Computational Social Systems* (2023).
- [5] Léon Bottou, Frank E Curtis, and Jorge Nocedal. 2018. Optimization methods for large-scale machine learning. *SIAM review* 60, 2 (2018), 223–311.

- [6] Pietro Buzzega, Matteo Boschini, Angelo Porrello, Davide Abati, and Simone Calderara. 2020. Dark experience for general continual learning: a strong, simple baseline. *Advances in neural information processing systems* 33 (2020), 15920–15930.
- [7] Francisco M Castro, Manuel J Marín-Jiménez, Nicolás Guil, Cordelia Schmid, and Karteek Alahari. 2018. End-to-end incremental learning. In *Proceedings of the European conference on computer vision (ECCV)*. 233–248.
- [8] Jiahua Dong, Hongliu Li, Yang Cong, Gan Sun, Yulun Zhang, and Luc Van Gool. 2023. No One Left Behind: Real-World Federated Class-Incremental Learning. *IEEE Transactions on Pattern Analysis and Machine Intelligence* (2023), 1–17. <https://doi.org/10.1109/TPAMI.2023.3334213>
- [9] Jiahua Dong, Lixu Wang, Zhen Fang, Gan Sun, Shichao Xu, Xiao Wang, and Qi Zhu. 2022. Federated class-incremental learning. In *Proceedings of the IEEE/CVF Conference on Computer Vision and Pattern Recognition*. 10164–10173.
- [10] Arthur Douillard, Matthieu Cord, Charles Ollion, Thomas Robert, and Eduardo Valle. 2020. Podnet: Pooled outputs distillation for small-tasks incremental learning. In *Computer Vision—ECCV 2020: 16th European Conference, Glasgow, UK, August 23–28, 2020, Proceedings, Part XX* 16. Springer, 86–102.
- [11] Arthur Douillard, Alexandre Ramé, Guillaume Couairon, and Matthieu Cord. 2022. Dytox: Transformers for continual learning with dynamic token expansion. In *Proceedings of the IEEE/CVF Conference on Computer Vision and Pattern Recognition*. 9285–9295.
- [12] Wenji He, Haipeng Yao, Tianle Mai, Fu Wang, and Mohsen Guizani. 2023. Three-stage Stackelberg game enabled clustered federated learning in heterogeneous UAV swarms. *IEEE Transactions on Vehicular Technology* (2023).
- [13] Saihui Hou, Xinyu Pan, Chen Change Loy, Zilei Wang, and Dahua Lin. 2019. Learning a unified classifier incrementally via rebalancing. In *Proceedings of the IEEE/CVF conference on Computer Vision and Pattern Recognition*. 831–839.
- [14] Xinting Hu, Kaihua Tang, Chunyan Miao, Xian-Sheng Hua, and Hanwang Zhang. 2021. Distilling causal effect of data in class-incremental learning. In *Proceedings of the IEEE/CVF conference on Computer Vision and Pattern Recognition*. 3957–3966.
- [15] Hyeonji Hwang, Seongjun Yang, Daeyoung Kim, Radhika Dua, Jong-Yeup Kim, Eunho Yang, and Edward Choi. 2023. Towards the practical utility of federated learning in the medical domain. In *Conference on Health, Inference, and Learning*. PMLR, 163–181.
- [16] Minsoo Kang, Jaeyoo Park, and Bohyung Han. 2022. Class-incremental learning by knowledge distillation with adaptive feature consolidation. In *Proceedings of the IEEE/CVF conference on computer vision and pattern recognition*. 16071–16080.
- [17] Sai Praneeth Karimireddy, Satyen Kale, Mehryar Mohri, Sashank Reddi, Sebastian Stich, and Ananda Theertha Suresh. 2020. Scaffold: Stochastic controlled averaging for federated learning. In *International conference on machine learning*. PMLR, 5132–5143.
- [18] James Kirkpatrick, Razvan Pascanu, Neil Rabinowitz, Joel Veness, Guillaume Desjardins, Andrei A Rusu, Kieran Milan, John Quan, Tiago Ramalho, Agnieszka Grabska-Barwinska, et al. 2017. Overcoming catastrophic forgetting in neural networks. *Proceedings of the national academy of sciences* 114, 13 (2017), 3521–3526.
- [19] Brian Lester, Rami Al-Rfou, and Noah Constant. 2021. The power of scale for parameter-efficient prompt tuning. *arXiv preprint arXiv:2104.08691* (2021).
- [20] Tian Li, Anit Kumar Sahu, Manzil Zaheer, Maziar Sanjabi, Ameet Talwalkar, and Virginia Smith. 2020. Federated optimization in heterogeneous networks. *Proceedings of Machine learning and systems* 2 (2020), 429–450.
- [21] Xiang Li, Kaixuan Huang, Wenhao Yang, Shusen Wang, and Zhihua Zhang. 2019. On the convergence of fedavg on non-iid data. *arXiv preprint arXiv:1907.02189* (2019).
- [22] Xiang Lisa Li and Percy Liang. 2021. Prefix-tuning: Optimizing continuous prompts for generation. *arXiv preprint arXiv:2101.00190* (2021).
- [23] Zhizhong Li and Derek Hoiem. 2017. Learning without forgetting. *IEEE transactions on pattern analysis and machine intelligence* 40, 12 (2017), 2935–2947.
- [24] Jiale Liu, Yu-Wei Zhan, Chong-Yu Zhang, Xin Luo, Zhen-Duo Chen, Yinwei Wei, and Xin-Shun Xu. 2023. Federated Class-Incremental Learning with Prompting. *arXiv preprint arXiv:2310.08948* (2023).
- [25] Mi Luo, Fei Chen, Dapeng Hu, Yifan Zhang, Jian Liang, and Jiashi Feng. 2021. No fear of heterogeneity: Classifier calibration for federated learning with non-iid data. *Advances in Neural Information Processing Systems* 34 (2021), 5972–5984.
- [26] Brendan McMahan, Eider Moore, Daniel Ramage, Seth Hampson, and Blaise Agüera y Arcas. 2017. Communication-efficient learning of deep networks from decentralized data. In *Artificial intelligence and statistics*. PMLR, 1273–1282.
- [27] Augustus Odena, Christopher Olah, and Jonathon Shlens. 2017. Conditional image synthesis with auxiliary classifier gans. In *International conference on machine learning*. PMLR, 2642–2651.
- [28] Ameya Prabhu, Philip HS Torr, and Puneet K Dokania. 2020. Gdumb: A simple approach that questions our progress in continual learning. In *Computer Vision—ECCV 2020: 16th European Conference, Glasgow, UK, August 23–28, 2020, Proceedings, Part II* 16. Springer, 524–540.
- [29] Daiqing Qi, Handong Zhao, and Sheng Li. 2023. Better generative replay for continual federated learning. *arXiv preprint arXiv:2302.13001* (2023).
- [30] Sylvestre-Alvise Rebuffi, Alexander Kolesnikov, Georg Sperl, and Christoph H Lampert. 2017. icarl: Incremental classifier and representation learning. In *Proceedings of the IEEE conference on Computer Vision and Pattern Recognition*. 2001–2010.
- [31] Hanul Shin, Jung Kwon Lee, Jaehong Kim, and Jiwon Kim. 2017. Continual learning with deep generative replay. *Advances in neural information processing systems* 30 (2017).
- [32] Neta Shoham, Tomer Avidor, Aviv Keren, Nadav Israel, Daniel Benditkis, Liron Mor-Yosef, and Itai Zeitak. 2019. Overcoming forgetting in federated learning on non-iid data. *arXiv preprint arXiv:1910.07796* (2019).
- [33] Christian Simon, Piotr Koniusz, and Mehrtash Harandi. 2021. On learning the geodesic path for incremental learning. In *Proceedings of the IEEE/CVF conference on Computer Vision and Pattern Recognition*. 1591–1600.
- [34] James Seale Smith, Leonid Karlinsky, Vyshnavi Gutta, Paola Cascante-Bonilla, Donghyun Kim, Assaf Arbelle, Rameswar Panda, Rogerio Feris, and Zsolt Kira. 2023. CODA-Prompt: COntinual Decomposed Attention-based Prompting for Rehearsal-Free Continual Learning. In *Proceedings of the IEEE/CVF Conference on Computer Vision and Pattern Recognition*. 11909–11919.
- [35] Yue Tan, Guodong Long, Lu Liu, Tianyi Zhou, Qinghua Lu, Jing Jiang, and Chengqi Zhang. 2022. Fedproto: Federated prototype learning across heterogeneous clients. In *Proceedings of the AAAI Conference on Artificial Intelligence*, Vol. 36. 8432–8440.
- [36] Anastasiia Usmanova, François Portet, Philippe Lalanda, and German Vega. 2021. A distillation-based approach integrating continual learning and federated learning for pervasive services. *arXiv preprint arXiv:2109.04197* (2021).
- [37] Ashish Vaswani, Noam Shazeer, Niki Parmar, Jakob Uszkoreit, Llion Jones, Aidan N Gomez, Łukasz Kaiser, and Illia Polosukhin. 2017. Attention is all you need. *Advances in neural information processing systems* 30 (2017).
- [38] Zifeng Wang, Zizhao Zhang, Sayna Ebrahimi, Ruoxi Sun, Han Zhang, Chen-Yu Lee, Xiaoqi Ren, Guolong Su, Vincent Perot, Jennifer Dy, et al. 2022. Dualprompt: Complementary prompting for rehearsal-free continual learning. In *European Conference on Computer Vision*. Springer, 631–648.
- [39] Zifeng Wang, Zizhao Zhang, Chen-Yu Lee, Han Zhang, Ruoxi Sun, Xiaoqi Ren, Guolong Su, Vincent Perot, Jennifer Dy, and Tomas Pfister. 2022. Learning to prompt for continual learning. In *Proceedings of the IEEE/CVF Conference on Computer Vision and Pattern Recognition*. 139–149.
- [40] Yue Wu, Yinpeng Chen, Lijuan Wang, Yuancheng Ye, Zicheng Liu, Yandong Guo, and Yun Fu. 2019. Large scale incremental learning. In *Proceedings of the IEEE/CVF Conference on Computer Vision and Pattern Recognition*. 374–382.
- [41] Jaehong Yoon, Wonyong Jeong, Giwoong Lee, Eunho Yang, and Sung Ju Hwang. 2021. Federated continual learning with weighted inter-client transfer. In *International Conference on Machine Learning*. PMLR, 12073–12086.
- [42] Jie Zhang, Chen Chen, Weiming Zhuang, and Lingjuan Lv. 2023. Addressing Catastrophic Forgetting in Federated Class-Continual Learning. *arXiv preprint arXiv:2303.06937* (2023).
- [43] Jie Zhang, Chen Chen, Weiming Zhuang, and Lingjuan Lyu. 2023. TARGET: Federated Class-Continual Learning via Exemplar-Free Distillation. In *Proceedings of the IEEE/CVF International Conference on Computer Vision*. 4782–4793.
- [44] Junting Zhang, Jie Zhang, Shalini Ghosh, Dawei Li, Serafettin Tasci, Larry Heck, Heming Zhang, and C-C Jay Kuo. 2020. Class-incremental learning via deep model consolidation. In *Proceedings of the IEEE/CVF Winter Conference on Applications of Computer Vision*. 1131–1140.

## Supplemental document for PIP: Prototypes-Injected Prompt for Federated Class Incremental Learning

This document offers supplementary materials for PIP: Prototypes-Injected Prompt for Federated Class Incremental Learning. Section A explains the derivation of the weighted aggregation of PIP. Section B presents the algorithm of the proposed baselines. Section C elaborates on a theoretical analysis of the proposed method that proves the convergence and generalization of PIP. Section D presents a detailed analysis of baseline complexity. The rest presents the detailed numerical results in various scenarios.

### A DERIVATION OF WEIGHTED AGGREGATION

Suppose that we have  $n$  samples of an observation  $x_i$  with the weight of  $w_i$ . The we mean and variance as:

$$\mu = \frac{1}{\sum_{i=1}^n w_i} \sum_{i=1}^n (x_i \cdot w_i) \quad (\text{A29})$$

$$\begin{aligned} \sigma^2 &= \frac{1}{\sum_{i=1}^n w_i} \sum_{i=1}^n w_i (x_i - \mu)^2 \\ &\approx \frac{1}{\sum_{i=1}^n w_i} \sum_{i=1}^n (w_i x_i^2 - w_i \mu^2) \end{aligned} \quad (\text{A30})$$

Or we have

$$\sum_{i=1}^n w_i \sigma^2 = \sum_{i=1}^n (w_i x_i^2 - w_i \mu^2) = \sum_{i=1}^n w_i x_i^2 - \sum_{i=1}^n w_i \mu^2 \quad (\text{A31})$$

that equal

$$\sum_{i=1}^n w_i \sigma^2 + \sum_{i=1}^n w_i \mu^2 = \sum_{i=1}^n w_i x_i^2 \quad (\text{A32})$$

If we have another  $m$  observation, then we have

$$\sum_{i=1}^{n+m} w_i \sigma^2 + \sum_{i=1}^{n+m} w_i \mu^2 = \sum_{i=1}^{n+m} w_i x_i^2 \quad (\text{A33})$$

$$\sum_{i=1}^{n+m} w_i \sigma^2 + \sum_{i=1}^{n+m} w_i \mu^2 = \sum_{i=1}^n w_i x_i^2 + \sum_{i=n+1}^{n+m} w_i x_i^2 \quad (\text{A34})$$

$$\sum_{i=1}^{n+m} w_i \sigma^2 + \sum_{i=1}^{n+m} w_i \mu^2 = \left( \sum_{i=1}^n w_i \sigma_{1:n}^2 + \sum_{i=1}^n w_i \mu_{1:n}^2 \right) + \left( \sum_{i=n+1}^{n+m} w_i \sigma_{n+1:m}^2 + \sum_{i=n+1}^{n+m} w_i \mu_{n+1:m}^2 \right) \quad (\text{A35})$$

$$\begin{aligned} \sum_{i=1}^{n+m} w_i \sigma^2 + \sum_{i=1}^{n+m} w_i \mu^2 &= \sum_{i=1}^n w_i (\sigma_{1:n}^2 + \mu_{1:n}^2) + \sum_{i=n+1}^{n+m} w_i (\sigma_{n+1:m}^2 + \mu_{n+1:m}^2) \\ &= \sum_{i=1}^n w_i (\sigma_{1:n}^2 + \mu_{1:n}^2) + \sum_{i=n+1}^{n+m} w_i (\sigma_{n+1:m}^2 + \mu_{n+1:m}^2) \end{aligned} \quad (\text{A36})$$

Therefore:

$$\sigma^2 = \frac{\sum_{i=1}^n w_i (\sigma_{1:n}^2 + \mu_{1:n}^2)}{\sum_{i=1}^{n+m} w_i} + \frac{\sum_{i=n+1}^{n+m} w_i (\sigma_{n+1:m}^2 + \mu_{n+1:m}^2) - \sum_{i=1}^{n+m} w_i \mu^2}{\sum_{i=1}^{n+m} w_i} \quad (\text{A37})$$

$$\begin{aligned} \sigma^2 &= \frac{\sum_{i=1}^n w_i (\sigma_{1:n}^2 + \mu_{1:n}^2)}{\sum_{i=1}^{n+m} w_i} + \frac{\sum_{i=n+1}^{n+m} w_i (\sigma_{n+1:m}^2 + \mu_{n+1:m}^2)}{\sum_{i=1}^{n+m} w_i} - \mu^2 \\ &= \frac{\sum_{i=1}^n w_i (\sigma_{1:n}^2 + \mu_{1:n}^2)}{\sum_{i=1}^{n+m} w_i} + \frac{\sum_{i=n+1}^{n+m} w_i (\sigma_{n+1:m}^2 + \mu_{n+1:m}^2)}{\sum_{i=1}^{n+m} w_i} - \mu^2 \end{aligned} \quad (\text{A38})$$

The derivation above shows that if we have two weighted Gaussian distributions e.g.  $X_1 \sim \mathcal{N}(\mu_1, \sigma_1^2)$  and  $X_2 \sim \mathcal{N}(\mu_2, \sigma_2^2)$  with total weight  $W_1 = \sum_{i=1}^{|X_1|} w_i$  and  $W_2 = \sum_{j=1}^{|X_2|} w_j$  respectively, then the aggregated distribution will be:

$$\mu^* = \frac{(\mu_1 \cdot W_1 + \mu_2 \cdot W_2)}{W_1 + W_2} \quad (\text{A39})$$

$$\sigma^{*2} = \frac{((\mu_1^2 + \sigma_1^2) \cdot W_1 + (\mu_2^2 + \sigma_2^2) \cdot W_2)}{W_1 + W_2} - \mu^{*2} \quad (\text{A40})$$

Generalizing equations above into  $N$  observations i.e.  $X_1 \sim \mathcal{N}(\mu_1, \sigma_1^2)$ ,  $X_2 \sim \mathcal{N}(\mu_2, \sigma_2^2)$ , ...  $X_N \sim \mathcal{N}(\mu_N, \sigma_N^2)$  with total weight  $W_1, W_2, \dots, W_N$  respectively, then the aggregated distribution will be:

$$\mu^* = \frac{\sum_{i=1}^N (\mu_i \cdot W_i)}{\sum_{i=1}^N W_i} \quad (\text{A41})$$

$$\sigma^{*2} = \frac{\sum_{i=1}^N (\mu_i^2 + \sigma_i^2) \cdot W_i}{\sum_{i=1}^N W_i} - \mu^{*2} \quad (\text{A42})$$

### B BASELINE ALGORITHM

We present the detailed algorithm of our proposed baseline in Algorithm 2.

### C DETAILED THEORETICAL ANALYSIS

Let  $\theta = (p, \phi)$  is the trainable parameters and  $F(\theta) = \mathbb{E}[\mathcal{L}_{l+}(\mathcal{T}; \theta)] = \mathbb{E}[\mathcal{L}_{l+}(\mathcal{T}; (p, \phi))]$  is the expected loss function,  $k, E, R$ , and  $L_S$  is local iteration, local epoch, global round, and number of selected local clients respectively. Please note that in this analysis,  $L_S$  denotes the number of selected local clients, while  $L \geq 1$  denotes a constant for  $L$ -smooth coefficient. We adopt the following assumptions adapted from SGD optimization convergence analysis [5] and FedAvg convergence analysis [21].

**Assumption 1:**  $F_1, \dots, F_L, \dots, F_{L_S}$  are all  $L$ -smooth: for all  $\theta$  and  $\theta'$ ,  $F_l(\theta) \leq F_l(\theta') + (\theta - \theta')^T \nabla F_l(\theta) + \frac{L}{2} \|\theta - \theta'\|_2^2$ .

**Assumption 2:**  $F_1, \dots, F_L, \dots, F_{L_S}$  are all  $\mu$ -strongly convex: for all  $\theta$  and  $\theta'$ ,  $F_l(\theta) \leq F_l(\theta') + (\theta - \theta')^T \nabla F_l(\theta) + \frac{\mu}{2} \|\theta - \theta'\|_2^2$ .

**Assumption 3:** Let  $\xi_l^k$  be the random uniformly sampled from  $l$ -th local data at  $k$ -th iteration. The variance of stochastic gradients in each client is bounded by:  $\mathbb{E}[\|\nabla F_l(\theta_l^k, \xi_l^k) - \nabla F_l(\theta_l^k)\|] \leq \sigma_l^2$  for  $l = 1, 2, \dots, L_S$ .

**Assumption 4:** The expected squared norm of stochastic gradients in each client is bounded by:  $\mathbb{E}[\|\nabla F_l(\theta_l^k, \xi_l^k)\|] \leq G^2$  for all  $l = 1, 2, \dots, L_S$  and  $k = 1, 2, \dots, K$  where  $K \in \mathbb{N}$ .

**Assumption 5:**  $\sum_{k=1}^{\infty} \alpha_l^k = \infty$  and  $\sum_{k=1}^{\infty} \alpha_l^{k2} < \infty$  where  $\alpha_l^k$  is the learning rate of  $l$ -th client in  $k$ -th step training.

#### C.1 Proof of Theorem 1

Suppose that a client  $S_l$  is trained locally with its local data  $\mathcal{T}_l^t \cup Z^t$ , where  $\mathcal{T}_l^t$  is local training samples for  $t$ -th task and  $Z^t$  is shared prototype for  $t$ -th task respectively. We already stated that  $Z^t$  contains augmented prototype so that  $|z_{c_2}^t| \approx |x_{c_1}|$  for  $z_{c_2}^t \in Z^t$  and  $x_{c_1}^t \in \mathcal{T}_{l_c}^t, T_{l_c}^t$  is subset of  $\mathcal{T}_l^t$  where  $y_i = c$  so the number of prototype of unavailable classes in  $\mathcal{T}_l^k$  and the samples of available classes in  $\mathcal{T}_l^k$  are balanced. Then the local model  $\theta_l = (p_l, \phi_l)$  is updated in  $K$  iteration based on sample  $\xi_l^k$  that sampled (e.g. minibatch) from  $\mathcal{T}_l^t \cup Z^t$ . Since the backbone (feature extractor)

**Algorithm 2** Fed-Prompt

---

```

1: Input: Number of clients  $N$ , number of selected local clients  $L$ , total number of rounds  $R$ , number of task  $T$ , local epochs  $E$ , batch size  $B$ .
2: Distribute frozen ViT backbone  $f$  to all clients  $\{S_l\}_{l=1}^N$  and central server  $S_G$ 
3: Initiate prompt, key, and head layer for all clients and central server  $p_G = p_l, \phi_G = \phi_l, l \in \{1..N\}$ 
4:  $R_T \leftarrow R/T$ ,  $R_T$  represents round per task
5: for  $t = 1 : T$  do
6:   for  $r = 1 : R_T$  do
7:      $S_l \leftarrow$  randomly select  $L$  local clients from  $N$  total clients
8:     Clients execute:
9:     Receive global parameters i.e. prompt and head layer  $p_G$  and  $\phi_G$ 
10:    Assign local parameters  $(p_l, \phi_l) \leftarrow (p_G, \phi_G)$ 
11:     $\mathcal{B} \leftarrow$  Split  $\mathcal{T}_l^t$  into  $B$  sized batches
12:    for  $e = 1 : E$  do
13:      for  $b = 1 : \mathcal{B}$  do
14:        Compute prompt-generated feature  $f_{p_l}(x)$  as in Eq. (1) to (4)
15:        Compute logits  $f_{\phi_l}(f_{p_l}(x))$ 
16:        Compute loss  $\mathcal{L}_t$  as in Eq. (5)
17:        Update local parameters  $(p_l, \phi_l)$  based on  $\mathcal{L}_t$  as in Eq. (6)
18:      end for
19:    end for
20:    Store local parameters  $(p_l, \phi_l)$ 
21:    Send local parameters  $(p_l, \phi_l)$  to server
22:    Server executes:
23:    Receives selected local clients  $S_l$  parameters  $(p_l, \phi_l)$  for  $l \in [1..L]$ 
24:    Aggregates clients' parameters into global parameters  $(p_G, \phi_G) \leftarrow \frac{1}{L} \sum_{l=1}^L (p_l, \phi_l)$ 
25:    Send global parameters  $(p_G, \phi_G)$  to clients for the next round
26:  end for
27: end for
28: Output: Global parameters  $(p_G, \phi_G)$  and local parameters  $(p_l, \phi_l), l \in 1..N$ 

```

---

is frozen, and  $\mathcal{T}_l^t \cup Z^t$  has balance samples for all classes, then  $\xi_l^k$  approximates  $\xi^k$  that is a sample from  $\mathcal{T}$ . The local model is updated by the stochastic gradient (SG) approach as presented in equations (6) and (10) in the main paper. Suppose that  $g(\theta_l, \xi_l^k)$  is the stochastic gradient function, then the update process can be simplified as:

$$\theta_l^{k+1} \leftarrow \theta_l^k - \alpha_l^k g(\theta_l^k, \xi_l^k) \quad (\text{A43})$$

Under assumption 1, and local training updates  $\theta$  by iterating SG with sample  $\xi_l^k$ , then we have:

$$\begin{aligned} F_l(\theta_l^{k+1}) - F_l(\theta_l^k) &\leq (\theta_l^{k+1} - \theta_l^k)^T \nabla F_l(\theta_l^k) + \frac{L}{2} \|\theta_l^{k+1} - \theta_l^k\|_2^2 \\ &\leq \nabla F_l(\theta_l^k)^T (\theta_l^{k+1} - \theta_l^k) + \frac{L}{2} \|\theta_l^{k+1} - \theta_l^k\|_2^2 \\ &\leq -\alpha_l^k \nabla F_l(\theta_l^k)^T g(\theta_l^k, \xi_l^k) + \alpha_l^{k2} \frac{L}{2} \|g(\theta_l^k, \xi_l^k)\|_2^2 \end{aligned} \quad (\text{A44})$$

The equation above can be derived into:

$$\begin{aligned} \mathbb{E}_{\xi_l^k} [F_l(\theta_l^{k+1})] - F_l(\theta_l^k) &\leq -\alpha_l^k \nabla F_l(\theta_l^k)^T \mathbb{E}[g(\theta_l^k, \xi_l^k)] \\ &\quad + \alpha_l^{k2} \frac{L}{2} \mathbb{E}_{\xi_l^k} [\|g(\theta_l^k, \xi_l^k)\|_2^2] \end{aligned} \quad (\text{A45})$$

The inequation above shows how SG optimizes  $\theta_l^k$  at a step  $k$ , and we can see clearly that the decreasing of  $F_l$  (left side) is bounded by a quantity in the right side involving  $\nabla F_l$  which is directional derivative of  $F_l$  at  $\theta_l^k$  along with  $-g(\theta_l^k, \xi_l^k)$  (first term) and second

moment of  $g(\theta_l^k, \xi_l^k)$  (second term). In the case where  $g(\theta_l^k, \xi_l^k)$  is unbiased estimator of  $\nabla F_l$ , then the inequation above can be derived as:

$$\mathbb{E}_{\xi_l^k} [F_l(\theta_l^{k+1})] - F_l(\theta_l^k) \leq -\alpha_l^k \nabla F_l(\theta_l^k)^T \mathbb{E}[g(\theta_l^k, \xi_l^k)] + \alpha_l^{k2} \frac{L}{2} \mathbb{E}_{\xi_l^k} [\|g(\theta_l^k, \xi_l^k)\|_2^2] \quad (\text{A46})$$

The inequation above shows that as long as the stochastic directions and stepsize are chosen, then the SGD convergence is guaranteed. To avoid the harm of the second term of the right side in the inequation above, we apply the restriction below

$$\mathbb{E}[g(\theta_l^k, \xi_l^k)] = \mathbb{E}[\|g(\theta_l^k, \xi_l^k)\|_2^2] - \|\mathbb{E}[g(\theta_l^k, \xi_l^k)]\|_2^2. \quad (\text{A47})$$

Adopting first and second-moment limit as in [5], then we add the following assumption.

**Assumption 6:** The objective function  $F_l$  and SG satisfy the following conditions.

- (a). The sequence of  $\{\theta_l^k\}$  is contained in an open space where  $F_l$  is bounded below by a scalar  $F_{inf}$
- (b) Exist scalars  $\nu_G \geq \nu > 0$  so that for all  $k \in \mathbb{N}$  satisfy:

$$\begin{aligned} \nabla F_l(\theta_l^k)^T \mathbb{E}_{\xi_l^k} [g(\theta_l^k, \xi_l^k)] &\geq \nu \|\nabla F_l(\theta_l^k)\|_2, \text{ and} \\ \|\mathbb{E}_{\xi_l^k} [g(\theta_l^k, \xi_l^k)]\|_2 &\leq \nu_G \|\nabla F_l(\theta_l^k)\|_2. \end{aligned} \quad (\text{A48})$$

- (c) Exist scalars  $m_1 \geq 0$  and  $m_2 \geq 0$  so that for all  $k \in \mathbb{N}$  satisfy:

$$\mathbb{E}[g(\theta_l^k, \xi_l^k)] \leq m_1 + m_2 \|\nabla F_l(\theta_l^k)\|_2 \quad (\text{A49})$$

Combining assumption 6 and restriction criteria as presented in equation (A19), then we have:

$$\begin{aligned} \mathbb{E}_{\xi_l^k} [\|g(\theta_l^k, \xi_l^k)\|_2^2] &\leq m_1 + m_G \|\nabla F_l(\theta_l^k)\|_2^2, \text{ with} \\ m_G &= m_2 + v_G^2 \geq v^2 > 0 \end{aligned} \quad (\text{A50})$$

Then by substituting  $\mathbb{E}_{\xi_l^k} [\|g(\theta_l^k, \xi_l^k)\|_2^2]$  from equation (A22) into equation (A17), we have:

$$\begin{aligned} \mathbb{E}_{\xi_l^k} [F_l(\theta_l^{k+1})] - F_l(\theta_l^k) &\leq -\alpha_l^k \nabla F_l(\theta_l^k)^T \mathbb{E}[g(\theta_l^k, \xi_l^k)] \\ &+ \alpha_l^{k^2} \frac{L}{2} (m_1 + m_G \|\nabla F_l(\theta_l^k)\|_2^2) \end{aligned} \quad (\text{A51})$$

Assumption 5 ensures that  $\{\alpha_l^k\} \rightarrow 0$  practically can be achieved by using learning rate decay that reduces learning rate in every step of local training. Then by choosing  $\alpha_l^k L m_G \leq v$  and substituting  $\nabla F_l(\theta_l^k)^T \mathbb{E}[g(\theta_l^k, \xi_l^k)]$  in equation (A23) with the condition in assumption 6.b, we have

$$\begin{aligned} \mathbb{E}_{\xi_l^k} [F_l(\theta_l^{k+1})] - F_l(\theta_l^k) &\leq -\alpha_l^k v \|\nabla F_l(\theta_l^k)\|_2^2 \\ &+ \alpha_l^{k^2} \frac{L}{2} (m_1 + m_G \|\nabla F_l(\theta_l^k)\|_2^2) \end{aligned} \quad (\text{A52})$$

Applying expectation to the equation above yield

$$\begin{aligned} \mathbb{E}_{\xi_l^k} [F_l(\theta_l^{k+1})] - \mathbb{E}[F_l(\theta_l^k)] &\leq -\alpha_l^k v \mathbb{E}[\|\nabla F_l(\theta_l^k)\|_2^2] \\ &+ \alpha_l^{k^2} \frac{1}{2} (m_1 + m_G \mathbb{E}[\|\nabla F_l(\theta_l^k)\|_2^2]) \\ \mathbb{E}_{\xi_l^k} [F_l(\theta_l^{k+1})] - \mathbb{E}[F_l(\theta_l^k)] &\leq -(\nu - \frac{1}{2} \alpha_l^k L m_G) \alpha_l^k \mathbb{E}[\|\nabla F_l(\theta_l^k)\|_2^2] \\ &+ \frac{1}{2} \alpha_l^{k^2} L m_1 \\ \mathbb{E}_{\xi_l^k} [F_l(\theta_l^{k+1})] - \mathbb{E}[F_l(\theta_l^k)] &\leq -\frac{1}{2} v \alpha_l^k \mathbb{E}[\|\nabla F_l(\theta_l^k)\|_2^2] \\ &+ \frac{1}{2} \alpha_l^{k^2} L m_1 \end{aligned} \quad (\text{A53})$$

Sum both sides for  $k \in \{1, \dots, K\}$  we get

$$\begin{aligned} F_{inf} - \mathbb{E}[F(\theta_l^1)] &\leq \mathbb{E}[F(\theta_l^{K+1})] - \mathbb{E}[F(\theta_l^1)] \\ F_{inf} - \mathbb{E}[F(\theta_l^1)] &\leq -\frac{1}{2} v \sum_{k=1}^K \alpha_l^k \mathbb{E}[\|\nabla F_l(\theta_l^k)\|_2^2] + \frac{1}{2} L m_1 \sum_{k=1}^K \alpha_l^{k^2} \end{aligned} \quad (\text{A54})$$

Dividing by  $v$  for both sides, then we get

$$\sum_{k=1}^K \alpha_l^k \mathbb{E}[\|\nabla F_l(\theta_l^k)\|_2^2] \leq \frac{2(\mathbb{E}[F(\theta_l^1)] - F_{inf})}{v} + \frac{L m_1}{v} \sum_{k=1}^K \alpha_l^{k^2} \quad (\text{A55})$$

Applying  $\lim_{K \rightarrow \infty}$  and assumption 5 to the equation above we get

$$\begin{aligned} \lim_{K \rightarrow \infty} \sum_{k=1}^K \alpha_l^k \mathbb{E}[\|\nabla F_l(\theta_l^k)\|_2^2] &\leq \frac{2(\mathbb{E}[F(\theta_l^1)] - F_{inf})}{v} \\ &+ \frac{L m_1}{v} \lim_{K \rightarrow \infty} \sum_{k=1}^K \alpha_l^{k^2} < \infty \end{aligned} \quad (\text{A56})$$

Dividing both sides with  $\sum_{k=1}^K \alpha_l^k$ , and following assumption 5 where  $\lim_{K \rightarrow \infty} \sum_{k=1}^K \alpha_l^k = \infty$  and  $\lim_{K \rightarrow \infty} \sum_{k=1}^K \alpha_l^{k^2} < \infty$ , then the right side will return 0. Therefore, we have

$$\lim_{K \rightarrow \infty} \frac{\sum_{k=1}^K \mathbb{E}[\alpha_l^k \|\nabla F_l(\theta_l^k)\|_2^2]}{\sum_{k=1}^K \alpha_l^k} = 0 \quad (\text{A57})$$

$$\lim_{K \rightarrow \infty} \mathbb{E} \left[ \frac{\sum_{k=1}^K \alpha_l^k \|\nabla F_l(\theta_l^k)\|_2^2}{\sum_{k=1}^K \alpha_l^k} \right] = 0 \quad (\text{A58})$$

$$\lim_{k \rightarrow \infty} \mathbb{E} [\|\nabla F_l(\theta_l^k)\|_2^2] = 0 \quad (\text{A59})$$

The equation above presents the convergence for local training in  $l$ -th client where the gradient of loss  $F$  converges to 0 along with the increase of training step/iteration  $k$ .

## C.2 Proof of Theorem 2

Suppose that set of local client  $\{S_l\}_{l=1}^{L_S}$  is trained locally with its local data  $\{\mathcal{T}_l^t \cup Z^t\}_{l=1}^{L_S}$ , where  $\mathcal{T}_l^t$  is local training sample for  $l$ -th client. Local training is conducted in  $k$  steps/iterations using a sample i.e. minibatch of local training set  $\xi_l^k \in \mathcal{T}_l^t$  on each step. Global synchronization is executed in each round  $r = \{1, 2, \dots, R\}$ . We global synchronization step as  $\mathcal{I}_E = \{rE | r = 1, 2, \dots, R\}$ . Following [21] we define  $\theta_l^{k+1}$  represents the local parameter of  $l$ -client after communication steps, while  $\vartheta_l^{k+1}$  represents the local parameter after an immediate result of one step SGD. Therefore the definition satisfies:

$$\vartheta_l^{k+1} = \theta_l^k - \alpha_l^k \nabla F_l(\theta_l^k, \xi_l^k) \quad (\text{A60})$$

$$\theta_l^{k+1} = \begin{cases} \vartheta_l^{k+1} & \text{if } k+1 \notin \mathcal{I}_E \\ \sum_{l=1}^{L_S} w_l \vartheta_l^{k+1} & \text{if } k+1 \in \mathcal{I}_E \end{cases} \quad (\text{A61})$$

Where  $w_l = \omega_l / \sum_{l=1}^{L_S} \omega_l$ , where  $\omega_l$  is the weight of  $l$ -th client. We define  $\bar{\vartheta}_l^{k+1} = \sum_{l=1}^{L_S} w_l \vartheta_l^{k+1}$  and  $\bar{\theta}_l^{k+1} = \sum_{l=1}^{L_S} w_l \theta_l^{k+1}$ ,  $\bar{\vartheta}_l^{k+1}$  is the result of single step SGD iteration from  $\bar{\theta}_l^{k+1}$ . We also define  $\bar{g}^k = \sum_{l=1}^{L_S} w_l \nabla F_l(\theta_l^k)$  and  $g^k = \sum_{l=1}^{L_S} w_l \nabla F_l(\theta_l^k, \xi_l^k)$ . We adopt the following lemmas from [21] where derived from fully participating clients in federated learning.

**Lemma 1:** By applying assumptions 1 and 2, in one step SGD training and chose  $\alpha \leq \frac{1}{4L}$  we have

$$\mathbb{E}[\|\bar{\vartheta}^{k+1} - \theta^*\|^2] \leq (1 - \alpha^k \mu) \mathbb{E}[\|\bar{\theta}^k - \theta^*\|^2] - (\alpha^k)^2 \mathbb{E}[\|g^k - \bar{g}^k\|^2] + 6L(\alpha^k)^2 \Gamma + 2\mathbb{E}[\sum_{l=1}^{L_S} w_l \|\bar{\theta}^k - \theta_l^k\|^2] \text{ where } \Gamma = F^* - \sum_{l=1}^{L_S} w_l F_l^* \geq 0.$$

**Lemma 2:** By applying assumption 3, the gradient function follows:  $\mathbb{E}[\|g^k - \bar{g}^k\|^2] \leq \sum_{l=1}^{L_S} w_l^2 \sigma_l^2$ , where  $\sigma_l^2$  is the variance of  $\theta_l$

**Lemma 3:** By applying assumption 4, where  $\alpha^k$  is non-increasing and it satisfies  $\alpha^k \leq \alpha^{k+E}$  for all  $k \geq 0$ , then we have  $\mathbb{E}[\|\bar{\theta}^{k+1} - \theta_l^k\|^2] \leq 4(\alpha^k)^2 (E-1)^2 G^2$

In fully participating clients we always have  $\bar{\theta}^{k+1} = \bar{\vartheta}^{k+1}$ . However, in partially participating clients we use a random sampling mechanism so that It satisfies  $\mathbb{E}_{S_L} [\bar{\theta}^{k+1}] = \bar{\vartheta}^{k+1}$ . We also adopt the bounding condition from [21] as shown in lemma 4.

**Lemma 4:** The expected different between  $\bar{\theta}^{k+1}$  and  $\bar{\vartheta}^{k+1}$  bounded by :  $\mathbb{E}_{S_L} [\|\bar{\theta}^{k+1} - \bar{\vartheta}^{k+1}\|^2] \leq \frac{4}{L_S} (\alpha^k)^2 E^2 G^2$  and in the case of  $w_l$  is uniform for all  $l$ -th client, then  $\mathbb{E}_{S_L} [\|\bar{\theta}^{k+1} - \bar{\vartheta}^{k+1}\|^2] \leq \frac{4(N_S - L_S)}{N_S - 1} (\alpha^k)^2 E^2 G^2$ , where  $N_S$  is total clients and  $L_S$  is number of selected clients.

Please note that

$$\|\bar{\theta}^{k+1} - \theta^*\|^2 = \|\bar{\vartheta}^{k+1} - \theta^*\|^2 \quad (\text{A62})$$

$$\|\bar{\vartheta}^{k+1} - \theta^*\|^2 = \|\bar{\theta}^{k+1} - \bar{\vartheta}^{k+1} + \bar{\vartheta}^{k+1} - \theta^*\|^2 \quad (\text{A63})$$

$$\begin{aligned} \|\bar{\theta}^{k+1} - \theta^*\|^2 &= \|\bar{\theta}^{k+1} - \bar{\vartheta}^{k+1}\|^2 + \|\bar{\vartheta}^{k+1} - \theta^*\|^2 \\ &+ 2\|\bar{\theta}^{k+1} - \bar{\vartheta}^{k+1}\| \cdot \|\bar{\vartheta}^{k+1} - \theta^*\| \end{aligned} \quad (\text{A64})$$

$$\begin{aligned} \|\bar{\theta}^{k+1} - \theta^*\|^2 &= \|\bar{\theta}^{k+1} - \bar{\theta}^{k+1}\|^2 + \|\bar{\theta}^{k+1} - \theta^*\|^2 \\ &\quad + 2\langle \bar{\theta}^{k+1} - \bar{\theta}^{k+1}, \bar{\theta}^{k+1} - \theta^* \rangle \end{aligned} \quad (\text{A65})$$

In the case of  $k+1 \notin \mathcal{I}_E$ , then the term  $\|\bar{\theta}^{k+1} - \bar{\theta}^{k+1}\|^2$  vanishes. Then by applying lemma 4, we get

$$\mathbb{E}[\|\bar{\theta}^{k+1} - \theta^*\|^2] \leq (1 - \alpha^k \mu) \mathbb{E}[\|\bar{\theta}^{k+1} - \theta^*\|^2] + (\alpha^k) B \quad (\text{A66})$$

In the case of  $k+1 \in \mathcal{I}_E$ , then by applying lemma 4, we get

$$\mathbb{E}[\|\bar{\theta}^{k+1} - \theta^*\|^2] \leq (1 - \alpha^k \mu) \mathbb{E}[\|\bar{\theta}^{k+1} - \theta^*\|^2] + (\alpha^k) (B+C) \quad (\text{A67})$$

where  $B = \sum_{l=1}^{L_S} w_l \sigma_l^2 + 6L\Sigma + 8(E-1)^2 G^2$  and  $C = \frac{4(N_S - L_S)}{N_S - 1} (E^2 G^2)$  if  $w_l$  is uniform and  $C = \frac{4}{L_S} (E^2 G^2)$  otherwise.

By choosing  $\alpha^k = \frac{\beta}{k+\delta}$  for some  $\beta > 1/\mu$  and  $\delta > 0$  so that  $\alpha^1 \leq \min\{1/\mu, 1/4L\} = 1/4L$  and  $\alpha^k \leq 2\alpha^{k+E}$  then we have  $\mathbb{E}[\|\bar{\theta}^{k+1} - \theta^*\|^2] \leq \frac{v}{\delta+k}$  where  $v = \max\{\frac{\beta^2(B+C)}{\beta\mu-1}, (\delta+1)\|\bar{\theta}^{k+1} - \theta^*\|^2\}$

Then, by applying a strong convexity assumption of  $F$  we have

$$\mathbb{E}[\bar{\theta}^k] - F^* \leq \frac{L}{2} \Delta^k \leq \frac{L}{2} \frac{v}{\delta+k} \quad (\text{A68})$$

where  $F^*$  is the minimum value of  $F$  where optimum parameter  $\theta^*$  is achieved. Later on, if we choose  $\beta = 2/\mu$ ,  $\delta = \max\{8L/\mu, E\}$  and denote  $\kappa = \theta$ . This shows that our idea i.e. injecting the shared prototypes improves model generalization.

$$\mathbb{E}[F(\bar{\theta}^k)] - F^* \leq \frac{\kappa}{(\delta+k-1)} \left( \frac{2(B+C)}{\mu} + \frac{\mu\delta}{2} \mathbb{E}[\|\theta^1 - \theta^*\|] \right) \quad (\text{A69})$$

The equation generalizes federated learning where the model is trained in a total of  $k$  steps/iterations where practical implementation satisfies  $k = b.E.R$ ,  $b$  is the number of batches. here we know that  $k > R$  as  $E$  and  $b$  are positive integers. Therefore, substituting  $k$  with  $R$  in the inequation above will produce a higher amount of the right side. Therefore, the inequation above can be generalized into:

$$\mathbb{E}[F(\bar{\theta}^R)] - F^* \leq \frac{\kappa}{(\delta+R-1)} \left( \frac{2(B+C)}{\mu} + \frac{\mu\delta}{2} \mathbb{E}[\|\theta^1 - \theta^*\|] \right) \quad (\text{A70})$$

The inequation above guarantees that to achieve a convergence condition in federated learning with weighted aggregation is upper bounded by the amount on the right side. The inequation above also shows the convergence guarantee by the method in the case of  $b = 1$  or  $E = 1$  or both, which simulates a small number of samples so that local training is only executed with 1 batch, or in an urgent (need to be fast) condition where local training is only executed with 1 epoch, or those two conditions occur in the same time.

### C.3 Proof of Theorem 3

Given  $\theta^*$  and  $\theta$  are optimal parameter in  $\mathcal{T}_l^t \cup Z^t$  and  $\mathcal{T}_l^t$  respectively, where  $\mathcal{T}_l^t \subset \mathcal{T}^t$ , where  $|\mathcal{T}_l^t|/|\mathcal{T}^t| = \eta \in (0, 1)$ , then we have

$$F(\theta; \mathcal{T}^t) = \eta F(\theta; \mathcal{T}_l^t) + (1 - \eta) F(\theta; (\mathcal{T}^t - \mathcal{T}_l^t)) \quad (\text{A71})$$

$$F(\theta^*; \mathcal{T}^t) = \eta F(\theta^*; \mathcal{T}_l^t) + (1 - \eta) F(\theta^*; (\mathcal{T}^t - \mathcal{T}_l^t)) \quad (\text{A72})$$

Suppose that  $\theta^o$  is the initial value both for  $\theta$  and  $\theta^*$  that set by random uniform initiation method. Therefore for all class  $c \in \mathcal{T}_c^t = \mathcal{T}_{y=c}^t$  It satisfy  $F(\theta^o; \mathcal{T}_c^t) = e^o$ . After optimally learning on  $\mathcal{T}_l^t$  and  $\mathcal{T}_l^t \cup Z^t$  then  $\theta^o$  become to  $\theta$  and  $\theta^*$  respectively. Please note that  $\theta$  learns only available class in  $\mathcal{T}_l^t$ , while  $\theta^*$  learns classes that available in  $\mathcal{T}_l^t$  and classes in  $\mathcal{T}^t - \mathcal{T}_l^t$  via  $Z^t$ . Suppose that

the loss for predicting classes in  $\mathcal{T}_l^t$  is defined as  $e^a < e^o$  then we have  $F(\theta; \mathcal{T}_l^t) = F(\theta^*; \mathcal{T}_l^t) = e^a < e^o$ . Since the backbone is frozen,  $\theta^*$  learn  $Z^t$  then we have  $F(\theta; (\mathcal{T}^t - \mathcal{T}_l^t)) = e^o$ , while  $F(\theta^*; (\mathcal{T}^t - \mathcal{T}_l^t)) = e^b$ , where  $e^a \geq e^b \geq e^o$ .

Then equation (A43) and (A44) can be derived to

$$F(\theta; \mathcal{T}^t) = \eta e^a + (1 - \eta) e^o \quad (\text{A73})$$

$$F(\theta^*; \mathcal{T}^t) = \eta e^a + (1 - \eta) e^b \quad (\text{A74})$$

Subtracting the equations above, then we have

$$F(\theta; \mathcal{T}^t) - F(\theta^*; \mathcal{T}^t) = \eta e^a + (1 - \eta) e^o - (\eta e^a + (1 - \eta) e^b) \quad (\text{A75})$$

$$F(\theta; \mathcal{T}^t) - F(\theta^*; \mathcal{T}^t) = \eta e^a + (1 - \eta) e^o - \eta e^a - (1 - \eta) e^b \quad (\text{A76})$$

$$F(\theta; \mathcal{T}^t) - F(\theta^*; \mathcal{T}^t) = (1 - \eta) e^o - (1 - \eta) e^b \quad (\text{A77})$$

$$F(\theta; \mathcal{T}^t) - F(\theta^*; \mathcal{T}^t) = (1 - \eta) (e^o - e^b) \quad (\text{A78})$$

Since  $0 < \eta < 1$  and  $e^o > e^b$  the right side of the inequation above has a positive value. By choosing a small positive value  $\epsilon > 0$  where  $(1 - \eta) (e^o - e^b) \geq \epsilon$  then we have.

$$F(\theta; \mathcal{T}^t) - F(\theta^*; \mathcal{T}^t) \geq \epsilon \quad (\text{A79})$$

Inequation above proves that  $\theta^*$  is more generalized to  $\mathcal{T}^t$  than  $\theta$ . This shows that our idea i.e. injecting the shared prototypes improves model generalization.

## D COMPLEXITY ANALYSIS

In this section, we analyze the complexity of our proposed baseline. Suppose that  $N_l$  is the total samples of a dataset of a client across all tasks,  $t \in \{1, \dots, T\}$  is task index,  $N_l^t = |\mathcal{T}_l^{t,t}| = |\mathcal{T}_l^t|$  is the number of samples on task  $t$  in client- $l$  that satisfy  $\sum_{t=1}^T N_l^t = N_l$ ,  $R$  is the total rounds of federated learning,  $E$  is the number of local epoch for each client training.  $\beta$  is the number of batches on each task that satisfy  $\sum_{b=1}^{\beta} N_{bl}^t = N_l^t$ . We simplify the derivation by analyzing the complexity in a common case that the tasks are divided evenly, therefore we have  $|\mathcal{T}_l^1| = |\mathcal{T}_l^2| = \dots = |\mathcal{T}_l^T| = |\mathcal{T}_l^T|$ , that equal  $N_l = T.N_l^t = T.|\mathcal{T}_l^t|$ . Let  $O(\cdot)$  denote the complexity of a process.

**Baseline Complexity:** Following the pseudo-code in Algorithm 2 then we have

$$O(\text{Baseline}) = O(1) + T.R_T.(O(\text{clients}) + O(\text{server})) \quad (\text{A80})$$

$$\begin{aligned} O(\text{Baseline}) &= O(1) + T.R_T.(L.O(1\text{client}) \\ &\quad + O(\text{server})) \end{aligned} \quad (\text{A81})$$

$$O(\text{Baseline}) = O(1) + T.R_T.(L.O(1\text{client}) + O(1)) \quad (\text{A82})$$

$$\begin{aligned} O(\text{Baseline}) &= O(1) + T.R_T.L.O(E. \sum_{b=1}^{\beta} N_{bl}^t + O(1)) \\ &\quad + O(T.R_T.) \end{aligned} \quad (\text{A83})$$

$$\begin{aligned} O(\text{Baseline}) &= O(1) + O(T.R_T.L.E. \sum_{b=1}^{\beta} N_{bl}^t) \\ &\quad + O(T.R_T.L.) + O(T.R_T) \end{aligned} \quad (\text{A84})$$

$$\begin{aligned} O(\text{Baseline}) &= O(T.R_T.L.E. \sum_{b=1}^{\beta} N_{bl}^t) \\ &\quad + O(T.R_T.L.) + O(T.R_T) \end{aligned} \quad (\text{A85})$$

From the definition above that  $\sum_{b=1}^{\beta} N_{bl}^t = N_l^t$ ,  $R_T = R/T$ ,  $N_l = T \cdot N_l^t = T$ , and  $L \geq 1$  therefore the complexity of the baseline will be

$$O(\text{Baseline}) = O(T \cdot R/T \cdot L \cdot E \cdot N_l^t) + O(T \cdot R/T \cdot L) + O(T \cdot R/T) \quad (\text{A86})$$

$$O(\text{Baseline}) = O(R \cdot L \cdot E \cdot N_l^t) + O(R \cdot L) + O(R) \quad (\text{A87})$$

$$O(\text{Baseline}) = O(R \cdot L \cdot E \cdot N_l^t) \quad (\text{A88})$$

Since  $N_l^t < N_l$  and  $E$  is set as a small constant in our method i.e. 2, then the baseline complexity will be:

$$O(\text{Baseline}) = O(R \cdot L \cdot N_l) \quad (\text{A89})$$

## E COMPLETE NUMERICAL RESULT OF ABLATION STUDY

In this section, we present the complete numerical result of the ablation study. Table A8 shows the detailed numerical result of PIP with various configurations in CIFAR100 dataset with T=10.

## F COMPLETE NUMERICAL RESULT OF EXPERIMENT ON 3 BENCHMARK DATASETS WITH T=5 AND T=20 SETTINGS

In this section, we present the detailed numerical results on different task sizes (T=5) and (T=20) on CIFAR100, MiniImageNet, and TinyImageNet datasets. Table A9 presents the complete numerical result

on CIFAR100 and MiniImageNet dataset with T=5 setting, while the complete numerical result on TinyImageNet dataset with T=5 is shown in Table A10. Table A11, A12, and A13 presents detailed numerical results with T=20 setting in CIFAR100, MiniImageNet, and TinyImageNet respectively.

## G COMPLETE NUMERICAL RESULT OF EXPERIMENT ON SMALLER LOCAL CLIENTS

In this section, we present the detailed numerical results of smaller local clients on CIFAR100, and TinyImageNet datasets. Table A14, and A15 presents detailed numerical results in CIFAR100, and TinyImageNet respectively with various numbers of selected local clients.

## H COMPLETE NUMERICAL RESULT OF EXPERIMENT ON SMALLER GLOBAL ROUNDS

In this section, we present the detailed numerical results of smaller global rounds on CIFAR100, and TinyImageNet datasets. Table A16, and A17 presents detailed numerical results in CIFAR100, and TinyImageNet respectively with various numbers of global rounds.

Received 20 February 2007; revised 12 March 2009; accepted 5 June 2009; revised 20 February 2007; revised 12 March 2009; accepted 5 June 2009

Config.	Prompt	Proto+Aug	W.Agg	Head	10	20	30	40	50	Avg	PD	Imp
A	✓				82.15	69.97	67.06	64.52	63.78	-	-	-
B	✓	✓			90.99	85.46	83.65	81.99	80.90	-	-	-
C	✓		✓		82.13	69.85	67.18	65.15	64.11	-	-	-
D	✓	✓	✓		91.37	86.46	84.37	82.79	81.87	-	-	-
E	✓			✓	96.60	83.20	77.10	74.08	70.86	-	-	-
F	✓	✓		✓	98.90	91.80	88.80	87.25	86.78	-	-	-
G	✓		✓	✓	98.60	71.80	68.73	67.68	68.44	-	-	-
PIP	✓	✓	✓	✓	<b>98.60</b>	<b>92.90</b>	<b>89.57</b>	<b>87.78</b>	<b>87.14</b>	-	-	-
Config.	Prompt	Proto+Aug	W.Agg	Head	60	70	80	90	100	Avg	PD	Imp
A	✓				62.99	62.72	61.90	61.12	60.66	65.69	21.49	22.59
B	✓	✓			79.07	78.63	78.99	78.69	77.56	81.59	<b>13.43</b>	6.69
C	✓		✓		63.50	62.84	62.78	62.16	61.35	66.10	20.78	22.18
D	✓	✓	✓		79.72	79.78	79.74	79.54	78.47	82.41	<b>12.90</b>	5.87
E	✓			✓	68.73	71.83	70.00	70.71	70.68	75.38	25.92	12.90
F	✓	✓		✓	85.52	85.29	84.83	84.86	84.17	87.82	14.73	0.46
G	✓		✓	✓	69.48	70.31	70.98	69.77	69.94	72.57	28.66	15.71
PIP	✓	✓	✓	✓	<b>85.93</b>	<b>85.60</b>	<b>85.45</b>	<b>85.22</b>	<b>84.60</b>	<b>88.28</b>	<b>14.00</b>	-

**Table A8: Complete numerical result of ablation study on CIFAR100 dataset (T=10) on one seeded run i.e. 2021. "Avg" denotes the average accuracy of all tasks, "PD" denotes performance drop, and "Imp" denotes improvement/gap of PIP compared to the respective configuration**

Method	CIFAR100 (T=5)								MiniImageNet (T=5)							
	20	40	60	80	100	Avg	PD	Imp	20	40	60	80	100	Avg	PD	Imp
iCaRL+FL	77.00	59.60	51.90	44.40	39.60	54.50	37.40	30.91	73.50	56.20	46.20	40.20	35.50	50.32	38.00	39.53
BiC+FL	78.40	60.40	53.20	47.50	41.20	56.14	37.20	29.27	72.60	56.80	49.20	43.50	38.70	52.16	33.90	37.69
PODNet+FL	77.60	62.10	56.30	50.80	43.30	58.02	34.30	27.39	73.10	58.40	53.20	46.50	43.40	54.92	29.70	34.93
DDE+iCaRL+FL	77.00	60.20	55.70	49.30	42.50	56.94	34.50	28.47	72.30	57.20	51.70	44.30	41.30	53.36	31.00	36.49
GeoDL+iCaRL+FL	72.50	61.10	54.00	49.50	44.50	56.32	28.00	29.09	71.80	59.60	52.30	46.10	42.50	54.46	29.30	35.39
SS-IL+FL	78.10	61.80	52.80	48.80	46.00	57.50	32.10	27.91	66.50	52.10	42.60	36.70	36.50	46.88	30.00	42.97
DyTox+FL	78.80	70.50	63.90	59.90	55.90	65.80	22.90	19.61	69.60	64.20	59.10	53.40	48.50	58.96	21.10	30.89
AFC+FL	71.10	63.80	58.40	53.60	46.40	58.66	24.70	26.75	78.00	64.50	57.00	51.30	47.30	59.62	30.70	30.23
GLFC	83.70	75.50	66.50	62.10	53.80	68.32	29.90	17.09	79.70	73.40	65.20	58.10	51.80	65.64	27.90	24.21
LGA	83.30	77.30	72.80	67.80	63.70	72.98	19.60	12.43	78.90	75.50	68.10	62.10	61.90	69.30	17.00	20.55
TARGET	77.10	39.08	26.95	20.71	17.72	36.31	59.38	49.10	61.75	28.48	18.33	11.95	7.58	25.62	54.17	64.23
Fed-L2P	89.50	69.70	63.33	59.89	58.35	68.15	31.15	17.26	91.40	77.38	74.03	72.73	74.91	78.09	16.49	11.76
Fed-DualP	93.15	76.88	67.55	66.56	66.06	74.04	27.09	11.37	94.35	81.13	74.67	73.51	76.67	80.06	17.68	9.79
<b>PIP-L2P</b>	92.55	<b>87.10</b>	<b>84.40</b>	<b>82.85</b>	<b>81.41</b>	<b>85.66</b>	<b>11.14</b>	<b>-0.25</b>	93.70	<b>89.83</b>	<b>88.97</b>	<b>88.45</b>	86.89	89.57	<b>6.81</b>	0.28
<b>PIP-DualP</b>	<b>96.75</b>	86.35	83.57	80.68	79.71	85.41	17.04	-	<b>95.30</b>	89.68	88.52	88.44	<b>87.32</b>	<b>89.85</b>	7.98	-

**Table A9: Complete numerical results on CIFAR100 and MiniImageNet dataset (T=5) in one-seeded run i.e. 2021**

TinyImageNet (T=5)								
Method	40	80	120	160	200	Avg	PD	Imp
iCaRL+FL	65.00	48.00	42.70	38.70	35.00	45.88	30.00	38.31
BiC+FL	65.70	48.70	43.00	40.30	35.70	46.68	30.00	37.51
PODNet+FL	66.00	50.30	44.70	41.30	37.00	47.86	29.00	36.33
DDE+iCaRL+FL	63.00	51.30	45.30	41.00	36.00	47.32	27.00	36.87
GeoDL+iCaRL+FL	65.30	50.00	45.00	40.70	36.00	47.40	29.30	36.79
SS-IL+FL	65.00	42.30	38.30	35.00	30.30	42.18	34.70	42.01
DyTox+FL	58.60	43.10	41.60	37.20	32.90	42.68	25.70	41.51
AFC+FL	62.50	52.10	45.70	43.20	35.70	47.84	26.80	36.35
GLFC	66.00	55.30	49.00	45.00	40.30	51.12	25.70	33.07
LGA	67.70	59.80	53.50	47.90	43.80	54.54	23.90	29.65
TARGET	53.25	27.08	17.77	11.04	7.28	23.28	45.97	60.91
Fed-L2P	82.70	70.23	66.33	62.51	63.73	69.10	18.97	15.09
Fed-DualP	85.10	67.23	60.25	55.99	58.59	65.43	26.51	18.76
PIP-L2P	82.70	70.23	66.33	62.51	63.73	69.10	18.97	15.09
PIP-DualP	<b>91.20</b>	<b>84.95</b>	<b>83.80</b>	<b>81.86</b>	<b>79.16</b>	<b>84.19</b>	<b>12.04</b>	<b>0.00</b>

Table A10: Complete numerical results on TinyImageNet dataset (T=5) in one seeded run i.e. 2021

CIFAR100 (T=20)													
Method	5	10	15	20	25	30	35	40	45	50	Avg	PD	Imp
iCaRL+FL	82.00	80.00	67.00	62.00	61.30	60.30	57.00	54.30	53.00	51.70	-	-	-
BiC+FL	82.00	77.30	68.30	64.00	63.70	62.30	60.30	58.70	55.00	53.30	-	-	-
PODNet+FL	83.00	76.30	70.30	68.00	66.30	67.00	65.30	61.70	61.30	58.70	-	-	-
DDE+iCaRL+FL	83.00	75.30	69.70	65.00	67.00	63.70	59.30	58.00	60.00	55.30	-	-	-
GeoDL+iCaRL+FL	82.00	78.30	71.30	67.70	68.00	65.30	64.30	60.00	58.70	56.00	-	-	-
SS-IL+FL	83.00	73.30	63.70	61.30	60.30	59.30	57.30	56.00	54.70	53.30	-	-	-
DyTox+FL	79.60	78.30	67.10	65.60	68.50	64.30	63.70	61.00	58.80	59.00	-	-	-
AFC+FL	75.60	69.60	57.10	58.50	45.50	55.40	51.40	50.40	45.20	42.40	-	-	-
GLFC	82.20	82.50	74.90	75.20	73.30	71.50	70.10	67.70	64.60	65.90	-	-	-
LGA	85.80	85.90	80.70	78.90	78.40	74.60	75.10	71.30	68.90	69.20	-	-	-
TARGET	34.20	15.70	9.93	8.60	4.64	3.90	3.23	2.72	2.56	1.86	-	-	-
Fed-L2P	94.00	87.70	74.13	74.70	74.36	71.90	74.06	72.40	71.71	68.96	-	-	-
Fed-DualP	94.80	91.40	85.13	85.00	84.20	80.17	79.14	76.75	76.60	75.46	-	-	-
PIP-L2P	94.60	88.70	80.07	76.85	72.76	69.83	68.97	67.97	67.91	65.82	-	-	-
PIP-DualP	<b>98.40</b>	<b>96.70</b>	<b>92.67</b>	<b>91.65</b>	<b>90.88</b>	<b>88.47</b>	<b>88.37</b>	<b>86.87</b>	<b>87.00</b>	<b>86.30</b>	-	-	-
Method	55	60	65	70	75	80	85	90	95	100	Avg	PD	Imp
iCaRL+FL	50.30	50.00	48.70	48.00	46.70	45.00	45.00	44.00	43.30	42.70	44.00	39.30	38.38
BiC+FL	52.00	51.30	50.30	49.70	48.00	47.00	46.30	45.70	45.30	44.30	45.72	37.70	36.66
PODNet+FL	56.30	55.00	54.00	53.00	51.00	50.30	49.30	48.00	48.30	47.70	48.72	35.30	33.66
DDE+iCaRL+FL	54.70	54.00	53.30	52.00	50.70	50.00	49.30	48.70	48.00	47.30	48.66	35.70	33.72
GeoDL+iCaRL+FL	55.30	55.00	53.70	53.00	51.70	50.70	50.00	49.00	49.30	48.00	49.40	34.00	32.98
SS-IL+FL	52.30	52.00	51.30	50.70	50.00	49.30	49.00	48.30	48.00	47.70	48.46	35.30	33.92
DyTox+FL	56.20	58.50	58.30	58.20	55.00	51.80	49.70	48.70	49.00	52.70	50.38	26.90	32.00
AFC+FL	41.30	35.60	37.10	37.80	38.90	35.20	34.40	34.50	36.20	33.80	34.82	41.80	47.56
GLFC	63.70	64.20	62.00	61.00	60.20	58.90	57.60	59.30	56.80	56.80	57.88	25.40	24.50
LGA	68.30	67.70	65.50	65.60	64.00	63.00	63.10	63.70	61.60	60.50	62.38	25.30	20.00
TARGET	1.45	1.03	1.42	1.57	1.71	1.38	1.67	2.13	2.19	1.94	1.86	32.26	80.52
Fed-L2P	68.95	66.90	65.52	66.56	64.68	65.20	63.56	64.81	63.00	62.46	63.81	31.54	18.57
Fed-DualP	75.60	72.80	71.92	72.37	70.89	70.94	71.16	71.11	70.89	70.30	70.88	24.50	11.50
PIP-L2P	63.02	60.37	59.14	58.21	59.39	59.51	62.15	63.06	61.72	60.33	61.35	34.27	21.03
PIP-DualP	<b>84.53</b>	<b>83.70</b>	<b>82.88</b>	<b>83.16</b>	<b>82.08</b>	<b>82.54</b>	<b>82.69</b>	<b>82.39</b>	<b>82.78</b>	<b>81.49</b>	<b>82.38</b>	<b>16.91</b>	-

Table A11: Complete numerical results on CIFAR100 dataset (T=20) in one-seeded run i.e. 2021

MinilImageNet (T=20)													
Method	5	10	15	20	25	30	35	40	45	50	Avg	PD	Imp
iCaRL+FL	83.00	66.00	61.30	56.00	56.30	53.00	49.70	47.00	46.30	46.00	-	-	-
BiC+FL	82.30	64.70	59.00	58.30	57.00	54.70	52.30	50.30	49.00	47.70	-	-	-
PODNet+FL	81.70	63.30	60.30	59.30	58.30	56.30	55.00	53.30	51.70	50.00	-	-	-
DDE+iCaRL+FL	80.00	60.70	58.70	56.30	57.00	55.30	53.00	51.70	50.30	49.30	-	-	-
GeoDL+iCaRL+FL	82.30	66.30	62.70	61.00	60.30	58.00	56.30	55.30	53.00	51.30	-	-	-
SS-IL+FL	80.00	65.30	61.70	57.30	56.30	54.00	51.30	50.00	49.30	48.30	-	-	-
DyTox+FL	71.60	52.70	61.60	53.20	56.80	48.90	45.70	49.40	39.10	44.10	-	-	-
AFC+FL	72.40	53.00	51.80	38.10	41.40	39.60	41.20	37.20	33.70	32.40	-	-	-
GLFC	84.00	71.70	70.00	69.30	67.30	66.30	61.00	60.70	59.30	58.70	-	-	-
LGA	78.80	79.40	76.80	73.50	69.80	68.50	67.30	66.10	63.80	62.10	-	-	-
TARGET	41.40	12.00	6.67	5.00	4.00	4.77	2.86	2.50	2.22	2.00	-	-	-
Fed-L2P	94.00	92.50	87.47	86.05	83.52	83.60	81.91	81.13	81.87	81.20	-	-	-
Fed-DualP	96.20	94.50	88.73	86.80	86.04	86.80	85.83	85.63	86.11	85.90	-	-	-
<b>PIP-L2P</b>	<b>94.20</b>	<b>92.10</b>	<b>90.80</b>	<b>89.05</b>	<b>86.92</b>	<b>86.77</b>	<b>85.49</b>	<b>84.20</b>	<b>85.84</b>	<b>83.94</b>	-	-	-
<b>PIP-DualP</b>	<b>97.80</b>	<b>96.70</b>	<b>94.33</b>	<b>92.45</b>	<b>91.92</b>	<b>91.70</b>	<b>91.09</b>	<b>90.80</b>	<b>91.07</b>	<b>90.34</b>	-	-	-
Method	55	60	65	70	75	80	85	90	95	100	Avg	PD	Imp
iCaRL+FL	44.00	42.30	40.00	39.70	37.30	36.00	34.70	34.30	33.00	32.00	34.00	51.00	54.17
BiC+FL	46.70	44.00	42.70	41.30	40.30	38.00	37.00	36.30	34.70	33.00	35.80	49.30	52.37
PODNet+FL	49.30	48.00	47.00	45.30	44.70	43.70	42.00	39.70	38.70	37.00	40.22	44.70	47.95
DDE+iCaRL+FL	48.70	48.30	47.70	46.70	45.70	44.30	42.30	40.00	38.30	37.30	40.44	42.70	47.73
GeoDL+iCaRL+FL	50.00	48.70	48.00	46.30	45.00	44.00	41.70	40.00	38.00	36.70	40.08	45.60	48.09
SS-IL+FL	47.00	45.00	44.30	43.00	41.30	40.70	39.30	38.70	37.00	36.00	38.34	44.00	49.83
DyTox+FL	37.70	35.20	33.60	31.50	28.60	27.30	27.10	26.50	25.80	24.90	26.32	46.70	61.85
AFC+FL	29.70	33.50	29.60	30.20	25.10	25.10	26.10	24.60	24.00	23.50	24.66	48.90	63.51
GLFC	55.30	53.00	52.00	50.30	49.70	47.30	46.00	42.70	40.30	39.00	43.06	45.00	45.11
LGA	60.60	59.80	57.20	56.80	55.10	54.70	54.10	53.20	51.60	48.20	52.36	30.60	35.81
TARGET	1.82	1.67	1.54	1.43	1.33	1.25	1.18	1.11	1.05	1.00	1.12	40.40	87.05
Fed-L2P	80.58	81.08	81.15	79.96	78.88	80.41	78.84	77.81	78.80	78.68	78.91	15.32	9.26
Fed-DualP	85.82	85.97	85.78	84.63	84.71	84.53	82.81	81.73	81.96	82.35	82.68	13.85	5.49
<b>PIP-L2P</b>	<b>83.16</b>	<b>82.95</b>	<b>82.86</b>	<b>81.56</b>	<b>79.69</b>	<b>79.91</b>	<b>79.59</b>	<b>78.14</b>	<b>80.23</b>	<b>78.85</b>	<b>79.35</b>	<b>15.35</b>	<b>8.82</b>
<b>PIP-DualP</b>	<b>89.69</b>	<b>90.03</b>	<b>89.97</b>	<b>89.43</b>	<b>89.20</b>	<b>89.14</b>	<b>88.38</b>	<b>87.39</b>	<b>87.89</b>	<b>88.04</b>	<b>88.17</b>	<b>9.76</b>	-

Table A12: Complete numerical results on MinilImageNet dataset (T=20) in one-seeded run i.e. 2021

TinyImageNet (T=20)													
Method	10	20	30	40	50	60	70	80	90	100	Avg	PD	Imp
iCaRL+FL	67.00	59.30	54.00	48.30	46.70	44.70	43.30	39.00	37.30	33.00	-	-	-
BiC+FL	67.30	59.70	54.70	50.00	48.30	45.30	43.00	40.70	38.00	33.70	-	-	-
PODNet+FL	69.00	59.30	55.00	51.70	50.00	46.70	43.70	41.00	39.30	38.00	-	-	-
DDE+iCaRL+FL	70.00	59.30	53.30	51.00	48.30	45.70	42.30	40.00	38.00	36.30	-	-	-
GeoDL+iCaRL+FL	66.30	56.70	51.00	49.70	44.70	42.30	41.00	39.00	37.30	35.00	-	-	-
SS-IL+FL	66.70	54.00	47.70	45.30	42.30	42.00	40.70	38.00	36.00	34.30	-	-	-
DyTox+FL	77.60	70.20	63.40	56.60	52.00	44.60	51.60	39.60	41.50	39.00	-	-	-
AFC+FL	74.00	62.90	57.60	54.20	45.10	44.40	40.70	36.90	33.00	33.60	-	-	-
GLFC	68.70	63.30	61.70	57.30	56.00	53.00	50.30	47.70	46.30	45.00	-	-	-
LGA	74.00	67.60	64.90	61.00	58.90	55.70	53.60	51.30	50.10	48.80	-	-	-
TARGET	28.00	12.40	7.67	7.40	5.60	3.67	2.63	2.12	1.93	1.88	-	-	-
Fed-L2P	75.60	72.50	74.80	74.60	72.64	74.97	74.66	74.70	73.49	70.94	-	-	-
Fed-DualP	79.40	78.90	79.00	78.10	76.48	77.53	77.14	76.85	76.04	75.48	-	-	-
<b>PIP-L2P</b>	<b>79.20</b>	<b>78.80</b>	<b>81.07</b>	<b>79.50</b>	<b>76.60</b>	<b>79.80</b>	<b>77.00</b>	<b>78.23</b>	<b>76.09</b>	<b>75.80</b>	-	-	-
<b>PIP-DualP</b>	<b>89.20</b>	<b>87.80</b>	<b>86.93</b>	<b>85.00</b>	<b>84.12</b>	<b>85.70</b>	<b>86.31</b>	<b>86.62</b>	<b>86.76</b>	<b>86.44</b>	-	-	-
Method	110	120	130	140	150	160	170	180	190	200	Avg	PD	Imp
iCaRL+FL	32.00	30.30	28.00	27.00	26.30	25.30	24.70	24.00	22.70	22.00	23.74	45.00	60.10
BiC+FL	32.70	32.30	30.30	29.00	27.70	27.30	26.00	25.70	24.30	23.30	25.32	44.00	58.52
PODNet+FL	37.00	35.70	34.70	34.00	33.00	32.30	31.00	30.00	29.30	28.00	30.12	41.00	53.72
DDE+iCaRL+FL	35.00	33.70	32.00	31.00	30.30	30.00	28.70	28.30	27.30	26.00	28.06	44.00	55.78
GeoDL+iCaRL+FL	33.70	32.00	31.00	30.30	28.70	28.00	27.30	26.30	25.00	24.70	26.26	41.60	57.58
SS-IL+FL	33.00	31.00	29.30	28.30	27.70	27.00	26.30	26.00	25.00	24.30	25.72	42.40	58.12
DyTox+FL	37.80	31.20	34.20	30.60	29.80	29.20	28.30	27.50	26.80	15.30	25.42	62.30	58.42
AFC+FL	30.80	28.90	27.10	22.80	24.50	23.60	22.10	20.70	18.40	18.10	20.58	55.90	63.26
GLFC	42.70	41.00	40.00	39.30	38.00	36.70	35.30	34.00	33.00	31.70	34.14	37.00	49.70
LGA	45.20	43.70	42.80	41.20	40.50	38.90	37.40	36.60	35.10	33.80	36.36	40.20	47.48
TARGET	1.69	1.48	1.26	1.27	1.17	1.02	0.66	0.60	0.53	0.50	0.66	27.50	83.18
Fed-L2P	71.35	70.38	70.46	67.47	67.20	65.20	66.16	65.23	68.61	65.94	66.23	9.66	17.61
Fed-DualP	75.20	75.37	75.23	73.90	73.76	72.80	73.27	72.20	72.28	71.69	72.45	7.71	11.39
<b>PIP-L2P</b>	<b>77.65</b>	<b>77.12</b>	<b>75.86</b>	<b>75.29</b>	<b>75.57</b>	<b>73.66</b>	<b>73.22</b>	<b>71.48</b>	<b>72.13</b>	<b>70.15</b>	<b>72.13</b>	<b>9.05</b>	<b>11.71</b>
<b>PIP-DualP</b>	<b>86.80</b>	<b>86.22</b>	<b>86.22</b>	<b>85.67</b>	<b>85.81</b>	<b>84.30</b>	<b>84.35</b>	<b>83.49</b>	<b>83.72</b>	<b>83.33</b>	<b>83.84</b>	<b>5.87</b>	-

Table A13: Complete numerical results on TinyImageNet dataset (T=20) in one-seeded run i.e. 2021

CIFAR100 (T=10)														
Method	#Local Clients (L)	10	20	30	40	50	60	70	80	90	100	AVG	PD	Imp
GLFC	10 (33.33%)	90.00	82.30	77.00	72.30	65.00	66.30	59.70	56.30	50.30	50.00	66.92	40.00	21.36
LGA	10 (33.33%)	89.60	83.20	79.30	76.10	72.90	71.70	68.40	65.70	64.70	62.90	73.45	26.70	14.83
TARGET	10 (33.33%)	65.10	37.15	26.50	21.25	19.00	16.43	14.40	13.19	11.38	10.03	23.44	55.07	64.84
Fed-L2P	10 (33.33%)	94.60	74.70	70.10	68.88	65.34	66.30	67.59	67.00	67.03	67.11	70.86	27.49	17.42
Fed-DualP	10 (33.33%)	96.60	83.20	77.10	74.08	70.86	68.73	71.83	70.00	70.71	70.68	75.38	25.92	12.90
PIP-L2P	10 (33.33%)	95.30	90.05	85.97	83.35	81.82	79.82	79.69	78.68	79.01	77.28	83.10	18.02	5.18
PIP-DualP	10 (33.33%)	<b>98.60</b>	<b>92.90</b>	<b>89.57</b>	<b>87.78</b>	<b>87.14</b>	<b>85.93</b>	<b>85.60</b>	<b>85.45</b>	<b>85.22</b>	<b>84.60</b>	<b>88.28</b>	<b>14.00</b>	<b>0.00</b>
GLFC	3 (10.00%)	86.70	74.50	71.70	65.63	65.26	60.37	54.51	52.63	48.30	44.56	62.42	42.14	24.64
LGA	3 (10.00%)	85.50	74.30	75.70	72.80	71.02	66.50	64.57	61.04	61.22	56.05	68.87	29.45	18.19
TARGET	3 (10.00%)	46.00	26.45	16.87	13.02	10.18	7.90	7.04	5.88	4.63	3.97	14.19	42.03	72.87
Fed-L2P	3 (10.00%)	80.40	74.20	73.77	71.00	71.30	69.65	68.29	69.04	69.44	72.33	71.94	8.07	15.12
Fed-DualP	3 (10.00%)	88.30	83.20	80.27	77.45	74.26	71.73	73.91	73.34	72.42	74.72	76.96	<b>13.58</b>	10.10
PIP-L2P	3 (10.00%)	94.50	84.80	80.30	78.30	73.70	70.47	67.34	66.60	67.18	67.62	75.08	26.88	11.98
PIP-DualP	3 (10.00%)	<b>98.40</b>	<b>92.00</b>	<b>90.57</b>	<b>89.03</b>	<b>87.72</b>	<b>83.30</b>	<b>83.69</b>	<b>82.71</b>	<b>82.36</b>	<b>80.88</b>	<b>87.06</b>	17.52	<b>0.00</b>
GLFC	2 (6.67%)	85.00	71.80	65.10	64.58	54.96	51.00	44.79	49.69	41.42	45.61	57.39	39.39	26.39
LGA	2 (6.67%)	86.40	76.35	78.07	67.75	63.40	62.67	61.57	56.61	60.39	53.61	66.68	32.79	17.10
TARGET	2 (6.67%)	49.70	24.60	16.67	12.45	9.80	7.53	6.74	5.41	4.69	4.20	14.18	45.50	69.60
Fed-L2P	2 (6.67%)	86.60	72.55	68.33	69.15	67.28	69.77	68.89	68.23	69.34	70.72	71.09	<b>15.88</b>	12.69
Fed-DualP	2 (6.67%)	90.10	76.95	71.93	71.40	68.14	69.55	69.14	67.66	67.93	68.92	72.17	21.18	11.61
PIP-L2P	2 (6.67%)	83.10	66.40	69.10	70.30	64.76	63.23	59.99	56.58	57.52	55.86	64.68	27.24	19.10
PIP-DualP	2 (6.67%)	<b>96.70</b>	<b>90.15</b>	<b>88.80</b>	<b>86.70</b>	<b>83.34</b>	<b>79.20</b>	<b>79.34</b>	<b>78.30</b>	<b>77.94</b>	<b>77.28</b>	<b>83.78</b>	19.42	<b>0.00</b>

Table A14: Complete numerical results on CIFAR100 (T=10) with smaller participating clients in one-seeded run i.e. 2021

TinyImageNet (T=10)														
Method	#Local Clients (L)	20	40	60	80	100	120	140	160	180	200	AVG	PD	Imp
GLFC	10 (33.33%)	66.00	58.30	55.30	51.00	47.70	45.30	43.00	40.00	37.30	35.00	47.89	31.00	38.90
LGA	10 (33.33%)	70.30	64.00	60.30	58.00	55.80	53.10	47.90	45.30	39.80	37.30	53.18	33.00	33.61
TARGET	10 (33.33%)	56.30	33.20	21.00	17.18	11.88	7.77	7.01	4.94	2.99	2.02	16.43	54.28	70.36
Fed-L2P	10 (33.33%)	80.80	74.40	72.53	70.53	67.24	68.62	67.99	67.93	65.70	64.50	70.02	16.30	16.77
Fed-DualP	10 (33.33%)	86.60	75.70	71.33	66.33	64.28	62.83	62.27	61.19	59.99	62.60	67.31	24.00	19.48
PIP-L2P	10 (33.33%)	85.40	84.55	83.57	84.73	83.66	84.30	82.90	81.61	80.31	77.51	82.85	<b>7.89</b>	3.94
PIP-DualP	10 (33.33%)	<b>92.70</b>	<b>87.90</b>	<b>86.83</b>	<b>88.23</b>	<b>87.04</b>	<b>87.18</b>	<b>85.96</b>	<b>85.13</b>	<b>84.62</b>	<b>82.35</b>	<b>86.79</b>	10.35	<b>0.00</b>
GLFC	3 (10.00%)	55.60	37.70	26.37	19.88	-	-	-	-	-	-	34.89	35.73	50.11
LGA	3 (10.00%)	73.30	69.55	60.30	52.75	47.16	-	-	-	-	-	60.61	26.14	24.39
TARGET	3 (10.00%)	36.70	20.20	12.37	8.60	5.06	3.53	2.89	2.00	1.26	0.80	9.34	35.90	75.66
Fed-L2P	3 (10.00%)	65.00	66.95	68.83	71.33	71.64	70.17	70.29	70.58	67.02	69.78	69.16	<b>-4.78</b>	15.84
Fed-DualP	3 (10.00%)	73.00	70.15	68.30	65.20	63.78	62.22	63.23	62.44	64.47	68.35	66.11	4.65	18.89
PIP-L2P	3 (10.00%)	82.60	83.35	81.20	82.95	80.24	80.17	79.04	75.99	76.36	70.39	79.23	12.21	5.77
PIP-DualP	3 (10.00%)	<b>90.40</b>	<b>87.10</b>	<b>85.03</b>	<b>86.90</b>	<b>85.92</b>	<b>85.05</b>	<b>83.64</b>	<b>82.64</b>	<b>82.40</b>	<b>80.95</b>	<b>85.00</b>	9.45	<b>0.00</b>
GLFC	2 (6.67%)	53.40	39.20	27.40	11.08	-	-	-	-	-	-	32.77	42.33	49.36
LGA	2 (6.67%)	71.40	59.75	57.17	54.43	49.96	-	-	-	-	-	58.54	21.44	23.59
TARGET	2 (6.67%)	34.40	16.85	10.67	5.80	2.72	1.53	1.16	0.92	0.84	0.68	7.56	33.72	74.57
Fed-L2P	2 (6.67%)	59.00	57.60	61.87	64.88	66.52	67.37	67.74	68.30	67.62	71.57	65.25	<b>-12.57</b>	16.88
Fed-DualP	2 (6.67%)	67.50	63.95	65.50	66.43	68.30	68.90	67.66	67.25	65.37	69.43	67.03	-1.93	15.10
PIP-L2P	2 (6.67%)	83.00	80.15	78.57	80.40	77.96	77.63	75.03	71.40	69.29	68.25	76.17	14.75	5.96
PIP-DualP	2 (6.67%)	<b>90.10</b>	<b>84.40</b>	<b>82.97</b>	<b>84.23</b>	<b>82.46</b>	<b>82.33</b>	<b>80.33</b>	<b>78.51</b>	<b>78.61</b>	<b>77.34</b>	<b>82.13</b>	12.76	<b>0.00</b>

Table A15: Complete numerical results on TinyImageNet (T=10) with smaller participating clients in one-seeded run i.e. 2021. GLFC and LGA performance is averaged from their first 4 and 5 tasks respectively due to crash

CIFAR100(T=10)												
Method	#Global Rounds (R)	10	20	30	40	50	60	70	80	90	100	Avg
GLFC(L=10)	100	90.00	82.30	77.00	72.30	65.00	66.30	59.70	56.30	50.30	50.00	66.92
LGA(L=10)	100	89.60	83.20	79.30	76.10	72.90	71.70	68.40	65.70	64.70	62.90	73.45
TARGET(L=10)	100	65.10	37.15	26.50	21.25	19.00	16.43	14.40	13.19	11.38	10.03	23.44
GLFC	100	86.70	74.50	71.70	65.63	65.26	60.37	54.51	52.63	48.30	44.56	62.42
LGA	100	85.50	74.30	75.70	72.80	71.02	66.50	64.57	61.04	61.22	56.05	68.87
TARGET	100	46.00	26.45	16.87	13.02	10.18	7.90	7.04	5.88	4.63	3.97	14.19
Fed-L2P	100	80.40	74.20	73.77	71.00	71.30	69.65	68.29	69.04	69.44	72.33	71.94
Fed-DualP	100	88.30	83.20	80.27	77.45	74.26	71.73	73.91	73.34	72.42	74.72	76.96
PIP-L2P	100	94.50	84.80	80.30	78.30	73.70	70.47	67.34	66.60	67.18	67.62	75.08
<b>PIP-DualP</b>	100	<b>98.40</b>	<b>92.00</b>	<b>90.57</b>	<b>89.03</b>	<b>87.72</b>	<b>83.30</b>	<b>83.69</b>	<b>82.71</b>	<b>82.36</b>	<b>80.88</b>	<b>87.06</b>
Fed-L2P	80	78.80	78.30	75.40	72.10	69.98	68.92	68.67	69.79	71.89	71.83	72.57
Fed-DualP	80	90.10	76.95	71.93	71.40	68.14	69.55	69.14	67.66	67.93	68.92	72.17
PIP-L2P	80	86.70	83.05	75.57	76.05	72.98	71.85	70.24	70.15	67.49	68.09	74.22
<b>PIP-DualP</b>	80	<b>96.70</b>	<b>90.15</b>	<b>88.80</b>	<b>86.70</b>	<b>83.34</b>	<b>79.20</b>	<b>79.34</b>	<b>78.30</b>	<b>77.94</b>	<b>77.28</b>	<b>83.78</b>
Fed-L2P	60	79.40	70.95	72.23	73.03	71.50	70.57	70.11	69.11	68.86	67.86	71.36
Fed-DualP	60	85.90	85.40	81.37	78.53	74.14	72.68	73.16	72.63	73.77	73.78	77.13
PIP-L2P	60	92.00	78.05	72.80	70.33	67.50	65.60	66.26	65.68	65.21	64.14	70.76
<b>PIP-DualP</b>	60	<b>97.60</b>	<b>91.40</b>	<b>87.03</b>	<b>86.10</b>	<b>85.36</b>	<b>82.13</b>	<b>82.00</b>	<b>81.69</b>	<b>80.80</b>	<b>80.15</b>	<b>85.43</b>
Fed-L2P	40	78.60	68.10	67.50	66.30	64.30	64.40	65.11	63.89	64.67	61.50	66.44
Fed-DualP	40	85.30	84.40	81.10	78.13	73.82	71.95	73.00	71.28	72.42	71.47	76.29
PIP-L2P	40	85.30	77.20	65.43	64.10	64.34	64.13	63.07	64.53	63.60	62.97	67.47
<b>PIP-DualP</b>	40	<b>97.70</b>	<b>93.65</b>	<b>88.13</b>	<b>86.38</b>	<b>84.20</b>	<b>82.97</b>	<b>82.26</b>	<b>81.36</b>	<b>81.27</b>	<b>79.87</b>	<b>85.78</b>
Fed-L2P	20	74.20	63.55	56.07	49.75	48.62	48.15	50.17	49.51	49.61	47.52	53.72
Fed-DualP	20	88.20	81.45	78.07	76.45	74.10	72.60	71.06	69.98	69.34	68.91	75.02
PIP-L2P	20	87.60	76.95	71.57	64.40	64.12	62.82	63.01	61.98	60.29	57.75	67.05
<b>PIP-DualP</b>	20	<b>97.80</b>	<b>91.05</b>	<b>86.40</b>	<b>83.33</b>	<b>83.42</b>	<b>81.27</b>	<b>81.13</b>	<b>82.01</b>	<b>81.01</b>	<b>80.28</b>	<b>84.77</b>

Table A16: Complete numerical results on CIFAR100 (T=10, local clients = 3) with smaller rounds in one-seeded run i.e. 2021

TinyImageNet(T=10)												
Method	#Global Rounds (R)	20	40	60	80	100	120	140	160	180	200	Avg
GLFC(L=10)	100	66.00	58.30	55.30	51.00	47.70	45.30	43.00	40.00	37.30	35.00	47.89
LGA(L=10)	100	70.30	64.00	60.30	58.00	55.80	53.10	47.90	45.30	39.80	37.30	53.18
TARGET(L=10)	100	56.30	33.20	21.00	17.18	11.88	7.77	7.01	4.94	2.99	2.02	16.43
GLFC	100	55.60	37.70	26.37	19.88	-	-	-	-	-	-	34.89
LGA	100	73.30	69.55	60.30	52.75	47.16	-	-	-	-	-	60.61
TARGET	100	36.70	20.20	12.37	8.60	5.06	3.53	2.89	2.00	1.26	0.80	9.34
Fed-L2P	100	65.00	66.95	68.83	71.33	71.64	70.17	70.29	70.58	67.02	69.78	69.16
Fed-DualP	100	86.60	75.70	71.33	66.33	64.28	62.83	62.27	61.19	59.99	62.60	67.31
PIP-L2P	100	82.60	83.35	81.20	82.95	80.24	80.17	79.04	75.99	76.36	70.39	79.23
<b>PIP-DualP</b>	100	<b>92.70</b>	<b>87.90</b>	<b>86.83</b>	<b>88.23</b>	<b>87.04</b>	<b>87.18</b>	<b>85.96</b>	<b>85.13</b>	<b>84.62</b>	<b>82.35</b>	<b>86.79</b>
Fed-L2P	80	65.00	68.55	71.20	71.30	71.12	71.87	73.04	73.66	72.28	73.03	71.10
Fed-DualP	80	74.80	72.05	71.60	70.08	68.14	66.72	66.63	65.80	65.57	71.81	69.32
PIP-L2P	80	82.20	83.15	82.37	83.65	82.00	80.18	78.39	77.03	76.82	74.39	80.02
<b>PIP-DualP</b>	80	<b>90.10</b>	<b>87.10</b>	<b>87.17</b>	<b>87.53</b>	<b>86.16</b>	<b>86.33</b>	<b>85.23</b>	<b>83.98</b>	<b>83.06</b>	<b>81.64</b>	<b>85.83</b>
Fed-L2P	60	66.20	70.30	71.77	74.25	72.90	73.77	74.47	73.05	72.36	71.15	72.02
Fed-DualP	60	73.40	73.10	72.07	70.60	69.30	67.68	66.69	67.60	66.43	71.02	69.79
PIP-L2P	60	79.70	79.70	80.60	80.20	79.50	79.43	75.39	73.98	72.87	70.13	77.15
<b>PIP-DualP</b>	60	<b>91.50</b>	<b>87.20</b>	<b>87.97</b>	<b>89.30</b>	<b>87.76</b>	<b>87.78</b>	<b>86.20</b>	<b>85.88</b>	<b>84.78</b>	<b>82.94</b>	<b>87.13</b>
Fed-L2P	40	70.20	72.95	72.53	74.28	74.58	73.78	73.33	71.13	71.03	70.37	72.42
Fed-DualP	40	72.30	72.05	73.27	71.60	71.48	69.70	68.74	67.20	67.26	69.40	70.30
PIP-L2P	40	80.20	78.60	77.67	79.78	78.10	76.27	75.87	72.15	71.92	70.42	76.10
<b>PIP-DualP</b>	40	<b>90.70</b>	<b>87.15</b>	<b>87.17</b>	<b>87.43</b>	<b>86.98</b>	<b>86.75</b>	<b>85.17</b>	<b>84.05</b>	<b>83.26</b>	<b>82.11</b>	<b>86.08</b>
Fed-L2P	20	61.00	59.45	63.23	64.85	65.10	65.03	62.39	60.35	59.19	57.15	61.77
Fed-DualP	20	73.90	75.55	75.10	74.28	72.44	72.75	71.51	69.45	68.78	70.71	72.45
PIP-L2P	20	80.20	78.15	77.43	77.83	76.12	76.85	74.14	73.64	71.77	67.18	75.33
<b>PIP-DualP</b>	20	<b>89.20</b>	<b>87.90</b>	<b>87.63</b>	<b>88.48</b>	<b>87.52</b>	<b>86.68</b>	<b>84.86</b>	<b>83.00</b>	<b>83.31</b>	<b>82.14</b>	<b>86.07</b>

Table A17: Complete numerical results on TinyImageNet (T=10, local clients = 3) with smaller rounds in one-seeded run i.e. 2021